Spin electric effects in molecular antiferromagnets

Mircea Trif,[1] Filippo Troiani,[2] Dimitrije Stepanenko,[1] and Daniel Loss[1]

[1]*Department of Physics, University of Basel, Klingelbergstrasse 82, CH-4056 Basel, Switzerland*
[2]*CNR-INFM National Research Center S3, Istituto Nanoscienze-CNR, via G. Campi 213/A, 41100 Modena, Italy*
(Received 24 January 2010; published 28 July 2010)

Molecular nanomagnets show clear signatures of coherent behavior and have a wide variety of effective low-energy spin Hamiltonians suitable for encoding qubits and implementing spin-based quantum information processing. At the nanoscale, the preferred mechanism for the control of a quantum systems is the application of electric fields, which are strong, can be locally applied, and rapidly switched. In this work, we provide the theoretical tools for identifying molecular nanomagnets suitable for electric control. By group-theoretical symmetry analysis we find that the spin-electric coupling in triangular molecules is governed by the modification of the exchange interaction and is possible even in the absence of spin-orbit coupling. In pentagonal molecules the spin-electric coupling can exist only in the presence of spin-orbit interaction. This kind of coupling is allowed for both $s=1/2$ and $s=3/2$ spins at the magnetic centers. Within the Hubbard model, we find a relation between the spin-electric coupling and the properties of the chemical bonds in a molecule, suggesting that the best candidates for strong spin-electric coupling are molecules with nearly degenerate bond orbitals. We also investigate the possible experimental signatures of spin-electric coupling in nuclear magnetic resonance and electron spin resonance spectroscopy, as well as in the thermodynamic measurements of magnetization, electric polarization, and specific heat of the molecules.

I. INTRODUCTION

The control of coherent quantum dynamics is a necessary prerequisite for quantum information processing. This kind of control is achieved through coupling of the internal quantum degrees of freedom of a suitable microscopic or mesoscopic system to an external classical or quantum field that can readily be manipulated on the characteristic spatial and temporal scales of the quantum system.

The molecular nanomagnets (MNs) (Refs. 1 and 2) represent a class of systems that show rich quantum behavior. At low energies, the MNs behave as a large spin or a system of only few interacting spins. The behavior of this spin system can be designed to some degree by altering the chemical structure of the molecules and ranges from a single large spin with high anisotropy barrier to small collections of ferromagnetically or antiferromagnetically coupled spins with various geometries and magnetic anisotropies. This versatility of available effective spin systems makes the MNs promising carriers of quantum information.[3] While the interaction with magnetic fields provides a straightforward access to the spins in an MN, it is preferable to use electric fields for the quantum control of spins since the electric fields are easier to control on the required short spatial and temporal scales. In this work, we explore the mechanisms of spin-electric coupling and study the ways in which an MN with strong spin-electric coupling can be identified.

Quantum behavior of MNs is clearly manifested in the quantum tunneling of magnetization.[4–11] A prototypical example of quantum tunneling of magnetization is the hysteresis loop of an MN with a large spin and high anisotropy barrier. The height of the barrier separating the degenerate states of different magnetization leads to long-lived spin configurations with nonzero magnetic moment in the absence of external fields. The transitions between magnetization states

in the MN driven through a hysteresis loop occur in tunneling events that involve coherent change in a many-spin state. These transitions have been observed as stepwise changes in magnetization in single-molecule ferromagnets.[7,8,12–14] Similar tunneling between spin configurations are predicted in antiferromagnetic molecules,[15,16] and the observed hysteresis was explained in terms of the photon bottleneck and Landau-Zener transitions.[17–20] The transitions between spin states are coherent processes and show the signatures of interference between transition paths,[21–23] as well as the effects of Berry phase in tunneling.[21–27]

Spin systems within molecular nanomagnets offer a number of attractive features for studying the quantum coherence and for the applications in quantum information processing.[3] A wide variety of spin states and couplings between them allows for encoding qubits. Chemical manipulation offers a way to modify the structure of low-energy spin states.[28] Coherence times of up to ~3 μs (Ref. 29) which can persist up to relatively high temperatures on the order of a few kelvin are sensitive to the isotopic composition of the molecule. A universal set of quantum gates can be applied in a system of coupled antiferromagnetic ring molecules, without the need for local manipulation.[30] The presence of many magnetic centers with the coupled spins allows for the construction of spin cluster qubits that can be manipulated by relatively simple means.[31] In polyoxometalates, the spin structure of the molecule is sensitive to the addition of charge, and controlled delivery and removal of charges via a scanning tunneling microscope (STM) tip can produce useful quantum gates.[32] Chemical bonds between the molecules can be engineered to produce the permanent coupling between the molecular spins and allow for interaction between the qubits.[33,34]

Sensitivity of molecular state to the addition of charge was demonstrated in the tunneling through single molecules[35] and used to control the spin state of a MN.[36]

Transport studies of the MNs can provide a sensitive probe of their spin structure.[27,37–40]

The most straightforward and traditional way of controlling magnetic molecules is by applying an external magnetic field. With carefully crafted electron spin resonance (ESR) pulses, it is possible to perform the Grover algorithm, or use the low-energy sector of the molecular nanomagnet as a dense classical memory.[3] Unfortunately, the approaches based on magnetic fields face a significant drawback in the large-scale quantum control application. Typically, the quantum manipulation has to be performed on very short spatial and temporal scales, while the local application of rapidly varying magnetic field presents a challenging experimental problem. For that reason, the schemes for quantum computing tend to rely on modifying the spin dynamics that is caused by intramolecular interaction, rather than on the direct manipulation of spins.[41]

The electric fields offer an attractive alternative for spin manipulation in the molecular nanomagnets.[42] One major advantage is that they can be applied to a very small volume via an STM tip[43,44] and rapidly turned on and off by applying voltage pulses to the electrodes placed close to the molecules that are being manipulated. Switchable coupling between different nanomagnets is essential for qubit implementation. At present, this can be implemented only locally, and the interaction is practically untunable. The use of microwave cavities can offer a solution to this problem. By placing the nanomagnets inside a microwave cavity, one can obtain a fully controllable, long-range interaction between them.[42] This coupling relies on the presence of a quantum electric field inside such a cavity, which mediates the interaction between distant nanomagnets. The interaction can be tuned by tuning each molecule in-or out-of-resonance with the cavity field using local electric or magnetic fields.[42] The spins, however, do not couple directly to the electric fields, classical or quantum, and therefore any electric spin manipulation is indirect and involves the modification of molecular orbitals or the spin-orbit interaction (SOI). Alternatively, the flying spin qubits can be manipulated by tailoring the exchange interactions and moving the domain walls in spin chains.[45,46]

The description of the molecular nanomagnets in terms of spins is an effective low-energy theory that does not carry information about the orbital states. However, it is still possible to predict the form of spin-electric coupling from symmetry considerations and single out the molecules in which such a coupling is possible. In particular, the molecules with the triangular arrangement of antiferromagnetically coupled spin-$1/2$ magnetic centers interact with external electric field through chirality of their spin structure.[42,47] The same coupling of chirality to the external electric field was derived for the triangular Mott insulators.[48]

While the symmetry of a molecule sets the form of spin-electric coupling, no symmetry analysis can predict the size of the corresponding coupling constant. The coupling strength will depend on the underlying mechanism that correlates the spin and orbital states, and on the detailed structure of low-energy molecular orbitals. To identify molecules that can be efficiently manipulated by electric fields, it is necessary to perform an extensive search among the molecules with the right symmetries and look for the ones that

also have a large coupling constant. Unfortunately, this search has to proceed by *ab initio* calculations of the coupling constants for a class of molecules of a given symmetry or by an indiscriminate experimental scanning of all of the available molecules.

We will consider the spin electric coupling in the language of effective model, namely, either the spin Hamiltonian or the Hubbard model. In reality the mechanism behind the spin-electric coupling involves either the modification of the electronic orbitals in an external field and the Coulomb repulsion of electrons or the much weaker direct spin-orbit coupling to the external fields. A derivation of spin-electric coupling from this realistic picture would require the knowledge of electronic orbitals from an *ab initio* calculation and the distribution of electric field within the molecule. Both of these problems require substantial computational power and cannot be performed routinely. Since the electric field acts primarily on the orbital degrees of freedom and the spin Hamiltonian carries no information about the orbital states, we provide a description in terms of a Hubbard model that still contains some information about the orbital states. We can then describe the properties of the molecule that allow for strong spin-electric coupling in the language of orbitals that offers some intuitive understanding of the underlying mechanisms of interaction.

The main body of the paper is divided into three largely independent sections that deal with the symmetry analysis, Hubbard model description, and experimental signatures of the spin-electric coupling. In Sec. II, we consider the general form of spin-electric coupling in the ring-shaped molecules. Based on the symmetry analysis, we identify the parameters of the spin Hamiltonian that can change in the electric field and cause spin-electric coupling. We find that the low-energy sector of the rings with odd number of spins (odd-spin rings) contains two Kramers doublets. Electric fields cause transitions between these states. The even-spin rings possess a nondegenerate $S=0$ ground state, making their low-energy sector unsuitable for electric manipulation. Among the odd-spin rings, we find that generically the triangular molecules show strongest coupling to electric fields. In triangles, the spin-electric coupling mechanism that is of the first order in electric field does not involve the spin-orbit coupling. Instead, the spin-electric coupling in the odd-spin rings with more than three spins requires it.

In Sec. III, we describe the molecules in terms of Hubbard model and find how the spin-electric coupling can be attributed to changes of Hubbard model parameters in the electric field. We show that the spin Hamiltonian description arises in the limit of spins well localized on the magnetic centers, and the symmetry-based results are confirmed in this limit. In addition, we consider a Hubbard model of a single superexchange bridge between magnetic centers. We find that the various symmetries of the bridge and the reduction in symmetry in external electric fields specifies the coupling between the spins on magnetic centers.

In Sec. IV, we identify the response of an MN with spin-electric coupling in the standard measurements of ESR, nuclear magnetic resonance (NMR), magnetization, polarization, linear magnetoelectric effect, and specific heat. Our conclusions are summarized in Sec. V.

II. SYMMETRY ANALYSIS OF ANTIFERROMAGNETIC SPIN RINGS

Spin chains whose ground state multiplet consists of two quasidegenerate $S=1/2$ doublets represent suitable candidates for the manipulation of the spin state by pulsed electric fields. Such a ground-state multiplet characterizes a number of frustrated spin rings, consisting of an odd number of half-integer spins. Rings containing an even number of antiferromagnetically coupled spins show no frustration, and in consequence the ground state is a nondegenerate $S=0$ state.

Symmetry analysis is one of the most powerful tools for investigating molecules. By identifying the point group symmetry associated with a given molecule, one can readily read the energy level structure of the system, as well as the allowed transitions induced by external perturbations. In even-spin molecular systems, the symmetry analysis is done by using the so called single-valued point groups.[49] In an odd-spin system instead, double valued point groups are usually used in order to describe the states, the splittings and the allowed transitions (magnetic or electric).[49] In the presence of spin-orbit interaction the splittings can be accounted for either by single group analysis (perturbatively) or by double group analysis (exact).

Using both the single group and double group analysis we pinpoint the transitions that arise in the absence or only in the presence of SOI. Therefore, the electric dipole transitions present in the single group are a consequence of the modified exchange interaction and can arise even in the absence of SOI, while the ones that show up only in the double group analysis are a consequence of the SOI (or modification of SOI in electric field).

We expect that the molecules that lack inversion symmetry are going to show stronger spin-electric coupling so that the odd-spin rings are the prime candidates for observing such effects. The importance of inversion stems from the fact that the electric field, being odd under inversion, can only cause transitions between the states of opposite parity in inversion symmetric molecules. Unless there is an accidental degeneracy, these transitions will be suppressed by an energy of the order of intramolecular exchange interaction. In the following we consider prototypical examples odd-spin ring systems and, in the Sec. II D, summarize the symmetry requirements for the existence of spin-electric coupling.

A. Triangle of $s=1/2$ spins

The low-energy properties of most molecular nanomagnets are well described in terms of spin degrees of freedom alone. Within the spin Hamiltonian approach, the coupling of external electric fields to the molecule can be accounted by suitably renormalizing the physical parameters. In the following, we use the symmetry of the molecules to calculate the changes of spin Hamiltonian parameters, to identify the system's eigenstates, and to deduce the allowed transitions. Quantitative estimates of the parameters entering the spin Hamiltonian require *ab initio* calculations[50] or comparison with experiments. The simplest example of a spin system which may couple to an external electric field in a nontrivial way is a triangle of $s=1/2$ spins, for example, the Cu_3
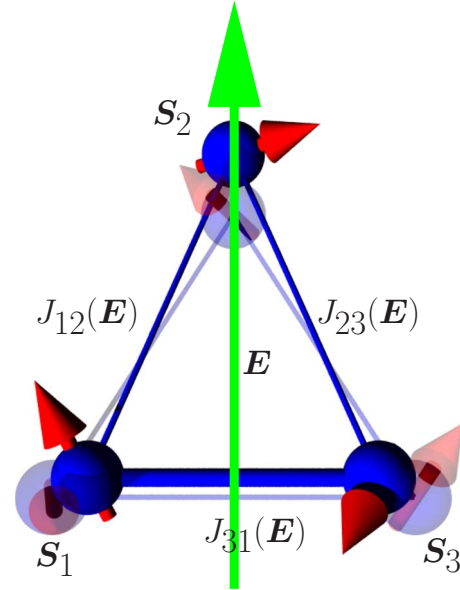

FIG. 1. (Color online) Schematics of the $s_i=1/2$ triangular molecule in electric field. The antiferromagnetic exchange couplings, represented by the bonds with thickness proportional to J_{ii+1}, are modified in electric field. In the absence of electric field, exchange couplings are equal $J_{ii+1}=J_{jj+1}$, here represented in gray (fade blue online). The black (blue online) triangle represents the exchange interaction strengths in electric field.

MN.[51,52] The schematics of such a spin system in the presence of an electric field is showed in Fig. 1. Its spin Hamiltonian, in the absence of external fields, reads:

$$H_{\text{spin}} = \sum_{i=1}^{N} J_{ii+1}\mathbf{s}_i \cdot \mathbf{s}_{i+1} + \sum_{i=1}^{N} \mathbf{D}_{ii+1} \cdot (\mathbf{s}_i \times \mathbf{s}_{i+1}), \quad (1)$$

with $N=3$ and $\mathbf{s}_4 \equiv \mathbf{s}_1$. The first term in Eq. (1) represents the isotropic Heisenberg exchange Hamiltonian with the exchange couplings J_{ii+1} between the spins $\mathbf{s}_i$ and $\mathbf{s}_{i+1}$, and the second term represents the Dzyalozhinsky-Moriya (DM) interaction due to the presence of SOI in the molecule, with the DM vectors $\mathbf{D}_{ii+1}$. The states of the spin triangle can be found by forming the direct product of the SU(2) representations of three spins $S=1/2$: $D_{tot}=D^{(1/2)\otimes 3}=2D^{(1/2)} \oplus D^{(3/2)}$, meaning there are eight states in total. The point group symmetry of the molecule is D_{3h},[51] which imposes the following restrictions on the spin Hamiltonian parameters: $J_{ii+1} \equiv J$ and $D_{ii+1}^{x,y} \equiv 0$, and $D_{ii+1}^z \equiv D_z$. The spin states in a form adapted to the rotational symmetry C_3 of the system are

$$|\psi_{M=1/2}^{(k)}\rangle = \frac{1}{\sqrt{3}} \sum_{j=0}^{2} \epsilon_j^k C_3^j |\downarrow\uparrow\uparrow\rangle, \quad (2)$$

$$|\psi_{M=3/2}\rangle = |\uparrow\uparrow\uparrow\rangle, \quad (3)$$

where $\epsilon_j = \exp(2i\pi j/3)$ and $j=0,1,2$. The states with opposite spin projection $M'=-M$, i.e., with all spins flipped can be written in an identical way (not shown). These states are already the symmetry adapted basis functions of the point

group D_{3h}. Moreover, these are eigenstates of the chirality operator

$$C_z = \frac{1}{4\sqrt{3}} \mathbf{s}_1 \cdot (\mathbf{s}_2 \times \mathbf{s}_3), \tag{4}$$

with $C_z |\psi_M^{(1,2)}\rangle = \pm |\psi_M^{(1,2)}\rangle$, $C_z |\psi_M^{(0)}\rangle = 0$, and $C_z |\psi_{M=\pm 3/2}\rangle = 0$. The above states in Eq. (3) carry different total spin. There are two spin $S=1/2$ states, corresponding to $k=1, 2$, and a spin $S=3/2$ state corresponding to $k=0$. Obviously, the states $|\psi_{M=\pm 3/2}\rangle$ have $S=3/2$.

Note that the quantum numbers $j=0, 1, 2$, and chirality $C_z = 0, \pm 1$ describe the same states. Since $\{e^{2i\pi C_z/3}\} \equiv \{e^{2i\pi j/3}\}$, we can use either of the two quantum numbers to classify the states. For an arbitrary $2n+1$ odd-spin chain with $n=1, 2, \ldots$ the same arguments hold. We can either use the set $\{e^{2i\pi k/3}\}$ with $k=0, 1, \ldots, 2n$, or $\{e^{2i\pi C_z/3}\}$ with $C_z = 0 \pm 1, \ldots, \pm n$ to quantify the states. The advantage of using one or another will show up in the next section when we treat the SOI.

1. Single valued group analysis of the $s=1/2$ spin triangle

In the single valued point group D_{3h}, the states $|\psi_{M=\pm 1/2}^{(k)}\rangle$ with $k=1, 2$ form the basis of the two dimensional irreducible representation E', while the states $|\psi_{M=\pm 1/2}^{(0)}\rangle$, and the $|\psi_{M=\pm 3/2}\rangle$ transform as A_2'. The allowed electric transitions in the system are determined by the transformation properties of the basis states.

The simplest and possibly the dominant dependence of the spin Hamiltonian on the applied electric field comes via the modification of the exchange interactions, like depicted in Fig. 1. This gives rise to the following term in the spin Hamiltonian:

$$\delta H_0(\mathbf{E}) = \sum_{i=1}^{3} \delta J_{ii+1}(\mathbf{E}) \mathbf{s}_i \cdot \mathbf{s}_{i+1}, \tag{5}$$

where $\delta J_{ii+1}(\mathbf{E}) \approx \mathbf{d}_{ii+1} \cdot \mathbf{E}$, with $\mathbf{d}_{ii+1}$ being vectors that describe the electric-dipole coupling of the bond $\mathbf{s}_i - \mathbf{s}_{i+1}$ to the electric field $\mathbf{E}$ in leading order. There are three such vector parameters and thus nine scalar parameters in total. However, symmetry will allow to drastically reduce the number of free parameters by providing relations between them. The $S=3/2$ states of the unperturbed spin Hamiltonian form the multiplet $^4A_2'$, while the $S=1/2$ states form two multiplets $^2E'$.[49] The electric dipole Hamiltonian is $H_{e-d} = -e\sum_i \mathbf{E} \cdot \mathbf{r}_i \equiv -e\mathbf{E} \cdot \mathbf{R}$, with e standing for the electron charge, $\mathbf{r}_i$ being the coordinates of the ith electron, and $\mathbf{R} = \sum_i \mathbf{r}_i$. The nonzero electric dipole matrix elements of H_{e-d} in the D_{3h} symmetric molecule are

$$\langle \psi_M^{(1,2)} | -eX | \psi_{M'}^{(2,1)}\rangle = i\langle \psi_M^{(1,2)} | -eY | \psi_{M'}^{(2,1)}\rangle \equiv d\delta_{MM'}, \tag{6}$$

proportional to the effective electric dipole parameter d. The value of d is not determined by symmetry and has to be found by some other means (*ab initio*, Hubbard modeling, experiments, etc.). All the other matrix elements are zero. The electric field acts only in the low-energy sector, which allows us to write the effective spin-electric coupling Hamiltonian acting in the lowest quadruplet as

$$H_{e-d}^{\text{eff}} = d\mathbf{E}' \cdot \mathbf{C}_\|, \tag{7}$$

where $\mathbf{E}' = \mathcal{R}_z(7\pi/6 - 2\theta)\mathbf{E}$, with $\mathcal{R}_z(\phi)$ describing the rotation with an angle ϕ about the z axis, and θ is the angle between in-plane component $\mathbf{E}_\|$ of the electric field $\mathbf{E}$ and the bond $s_1 - s_2$. For $\mathbf{C}_\| = (C_x, C_y, 0)$ we have

$$C_x = \sum_M (|\psi_M^{(1)}\rangle\langle\psi_M^{(2)}| + |\psi_M^{(2)}\rangle\langle\psi_M^{(1)}|), \tag{8}$$

$$C_y = i\sum_M (|\psi_M^{(1)}\rangle\langle\psi_M^{(2)}| - |\psi_M^{(2)}\rangle\langle\psi_M^{(1)}|). \tag{9}$$

The low-energy spectrum in the presence of electric field and the related states can be expressed in terms of the spin Hamiltonian Eq. (5) so that we find anisotropic variations of the exchange coupling constants,

$$\delta J_{ii+1}(\mathbf{E}) = \frac{4d}{3} |\mathbf{E}_\|| \cos\left(\frac{2\pi}{3} i + \theta\right), \tag{10}$$

which depend on the angle θ and the projection of the electric field $\mathbf{E}$ on the plane of the triangle. In the $s_i = 1/2$ triangle the $\mathbf{C}$ operators can be written as

$$C_x = -\frac{2}{3}(\mathbf{s}_1 \cdot \mathbf{s}_2 - 2\mathbf{s}_2 \cdot \mathbf{s}_3 + \mathbf{s}_3 \cdot \mathbf{s}_1), \tag{11}$$

$$C_y = \frac{2}{\sqrt{3}}(\mathbf{s}_1 \cdot \mathbf{s}_2 - \mathbf{s}_3 \cdot \mathbf{s}_1), \tag{12}$$

with $[C_i, C_j] = 2i\epsilon_{ijk}C_k$ (ϵ_{ijk} are the Levi-Civita symbols).[42,48] From the above relations we can conclude that (i) only the electric field component perpendicular to the bond and lying in the plane of the molecule gives rise to spin-electric coupling; (ii) there is only one free parameter d describing the coupling of the spin system to electric fields and $\mathbf{d}_{ii+1} = 4d/3 [\sin(2i\pi/3), \cos(2i\pi/3), 0]$.

The SOI in a D_{3h} symmetric MN is constrained by the transformation properties of the localized orbitals. It reads

$$H_{\text{SO}} = \lambda_{\text{SO}}^\| T_{A_2} S_z + \lambda_{\text{SO}}^\perp (T_{E_+''} S_- + T_{E_-''} S_+), \tag{13}$$

with T_Γ being tensor operators transforming according to the irreducible representation Γ.[49] The nonzero matrix elements of this SOI Hamiltonian in the low-energy quadruplet read $\langle \psi_M^{(1,2)} | H_{\text{SO}} | \psi_{M'}^{(1,2)}\rangle = \pm M\lambda_{\text{SO}}^\| \delta_{MM'}$ so that the SOI takes the following effective form:

$$H_{\text{SO}} = \Delta_{\text{SO}} C_z S_z, \tag{14}$$

with $\Delta_{\text{SO}} = \lambda_{\text{SO}}^\|$ and $S_z = \sum_i^3 s_i^z$. An effective SOI Hamiltonian is obtained also from the DM SOI Hamiltonian in Eq. (1). The constraints $D_{ii+1}^{x,y} = 0$ and $D_{ii+1}^z \equiv D_z$ on the DM vectors due to D_{3h} symmetry of the molecule give rise to the same effective SOI in Eq. (14), with $D_z = \lambda_{\text{SO}}^\|$. Thus, as expected, the molecular SOI and the DM SOI give rise to the same effective SOI Hamiltonian acting in the low energy quadruplet. Like in the case of the electric dipole parameter d, finding $D_z(\lambda_{\text{SO}}^\|)$ requires more than symmetry, like *ab initio* methods or experiments. The transverse SOI, with interaction strength $\lambda_{\text{SO}}^\perp$ does not act within the low-energy space, and its effect will
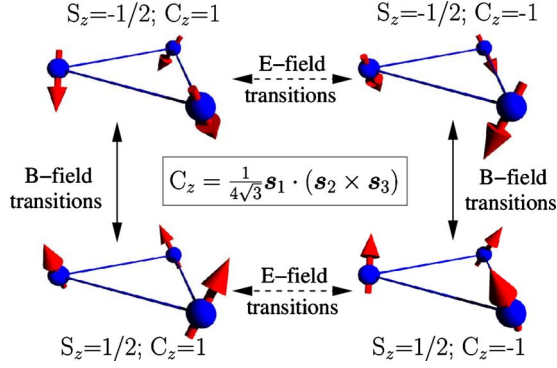
FIG. 2. (Color online) The spin transitions in the $s_i=1/2$ triangle induced by electric and magnetic fields. The electric field causes transitions between the states of opposite chiralities C_z and equal spin projections S_z (horizontal arrows), while the magnetic field instead causes transitions between the states of opposite spin projections S_z and equal chiralities C_z (vertical arrows).

appear only in higher orders of perturbation theory in $\lambda_{SO}^{\perp}/J$.

An external magnetic field couples to the spin via the Zeeman term $H_Z = \mathbf{B} \cdot \bar{\bar{g}} \mathbf{S}$, with $\bar{\bar{g}} = \text{diag}\{g_{\parallel}, g_{\parallel}, g_{\perp}\}$ being the g-factor tensor in D_{3h}. The full effective Hamiltonian describing the low-energy quadruplet in the presence of SOI, electric field, and magnetic field reads

$$H_{\text{eff}} = \Delta_{SO} C_z S_z + \mathbf{B} \cdot \bar{\bar{g}} \mathbf{S} + d\mathbf{E}' \cdot \mathbf{C}_{\parallel}. \tag{15}$$

Note that $[\mathbf{C}, \mathbf{S}] = 0$, and chirality and spin act as independent spin 1/2 degrees of freedom. Furthermore, in the absence of SOI the chirality $\mathbf{C}$ and the spin $\mathbf{S}$ evolve independently. However, the SOI couples the two and provides with means for electric control of both spin and chirality. Vice versa, magnetic fields can also couple to chirality due to SOI. Also, while magnetic fields (time-dependent) cause transitions between states of opposite spin projection M but with the same chirality C_z, the electric field does the opposite: it causes transitions between states of opposite chirality C_z, but carrying the same M. Full control of the lowest quadruplet is thus realized in the presence of both electric and magnetic fields, as can be seen in Fig. 2.

2. Double valued group states of the s=1/2 spin triangle

The double groups provide a formalism that takes into account the fact that the rotation of a half-integer spin by the angle 2π does not produce the identity transformation on its quantum state. The double group representations allow to nonperturbatively describe the magnetic and electric transitions in the presence of spin-orbit interaction (see Chapter 10 of Ref. 49). The lowest quadruplet consists of two Kramers doublets, transforming like $\bar{E}'$ and $\bar{E}''$, respectively. The $S=3/2$ states transform as $\bar{E}'$ (for $M=\pm 1/2$) and $\bar{E}''$ ($M=\pm 3/2$). Thus, the $S=1/2$ states mix with the $S=3/2$ states, but only the ones transforming according to the same representations, i.e., there is no mixing between $\bar{E}'$ and $\bar{E}''$ due to spin-orbit interaction. The magnetic dipole transitions take place between $\bar{E}'$ and $\bar{E}''$, and within $\bar{E}'$ and $\bar{E}''$, respectively, while electric dipole transitions take place only between $\bar{E}'$

and $\bar{E}''$. The selection rules for the electric transitions are $\Delta M = \pm 2$, while for the magnetic transitions these are $\Delta M = 0, \pm 1$. We see that there are allowed electric dipole transitions also within the $S=3/2$ subspace.

We can now establish several selection rules for the SOI, electric field, and magnetic field induced transitions. Note that the above analysis was exact in SOI. However, it instructive to treat electric field, magnetic fields, and SOI on the same footing. First, we find that the electric dipole transitions fulfill the selection rules $\Delta C_z = \pm 1$ and $\Delta S_z = 0$, meaning that electric field only couples states within the lowest quadruplet. The SOI transitions show a richer structure. We can separate the SOI interaction in two parts: the perpendicular SOI, quantified by D_z in the DM interaction Hamiltonian, and the in-plane SOI, quantified by $D_{x,y}$ in the DM interaction Hamiltonian, respectively. By doing so, we find that the D_z SOI terms obey the selections rules $\Delta C_z = 0$ and $\Delta S_z = 0$, while for the $D_{x,y}$ terms we get the selection rules $\Delta C_z = \pm 1$ and $\Delta S_z = \pm 1$. Due to the cyclic boundary conditions the relation $C_z = 1 + 1 \equiv C_z = -1$ holds. Moreover, for a $2n+1$ spin ring with $n = 1, 2, \ldots$, this relation is generalized to $C_z = n + 1 \equiv C_z = -n$. We see that in-plane SOI ($D_{x,y}$ terms) do not cause any splitting in the ground state and can lead to observable effects only in second order in perturbation theory in $D_{x,y}/J$. Also, note that if σ_h symmetry is present, $D_{x,y} \equiv 0$ and thus there are no in-plane SOI effects at all. Modification of these terms due to an in-plane external electric field $\mathbf{E}$, however, lead to different selection rules: changes in D_z terms lead to $\Delta C_z = \pm 1$ and $\Delta S_z = 0$, while modification of $D_{x,y}$ lead to $\Delta C_z = 0, \pm 2$ and $\Delta S_z = \pm 1$. The magnetic field transitions obey the selection rules $\Delta S_z = 0, \pm 1$ and $\Delta C_z = 0$. Thus, we can make clear distinction between pure electric field transitions, SOI-mediated electric transitions, and magnetic transitions. This distinction between the electric and magnetic field induced transitions could be used to extract the spin-electric coupling strength parameter d from spectroscopic measurements.

B. Spin $s=3/2$ triangle

The spin $s=3/2$ triangle has a more complex level structure than the $s=1/2$ triangle due to its higher spin. The spin Hamiltonian, however, is similar to the one in Eq. (1) for $s=1/2$, and the reduction in the representation of three spins $S=3/2$ is $D_{tot} = D^{(3/2)\otimes 3} = 2D^{(1/2)} \oplus 4D^{(3/2)} \oplus 3D^{(5/2)} \oplus 2D^{(7/2)} \oplus D^{(9/2)}$, a total of 64 spin states. The $s=3/2$ triangle states can be defined according to their transformation properties under threefold rotations C_3 in D_{3h} and are of the following form:

$$|\psi_M^{(k,i)}\rangle = P_k^3 |M, i\rangle, \tag{16}$$

$$P_k^3 = \frac{1}{\sqrt{3}} \sum_{j=0}^{2} \epsilon_j^k C_3^j, \tag{17}$$

where $\epsilon_j^k = \exp(2i\pi jk/3)$, C_3^j are the threefold rotation of order j, and $j, k = 0, 1, 2$. The states $|M, i\rangle \equiv |\sigma_1 \sigma_2 \sigma_3\rangle$ represent all possible states (i states in total) with a given spin projection $M(\equiv \Sigma_k \sigma_k)$ that cannot be transformed into each other

TABLE I. Nonsymmetry adapted states of the $s=3/2$ spin triangle. We use $|\Uparrow(\Downarrow)\rangle=|\pm3/2\rangle$ and $|\uparrow(\downarrow)\rangle=|\pm1/2\rangle$.

M	i			
	1	2	3	4
$1/2$	$|\downarrow\uparrow\uparrow\rangle$	$|\Uparrow\downarrow\downarrow\rangle$	$|\Downarrow\Uparrow\uparrow\rangle$	$|\Downarrow\uparrow\Uparrow\rangle$
$3/2$	$|\Downarrow\Uparrow\Uparrow\rangle$	$|\downarrow\uparrow\Uparrow\rangle$	$|\downarrow\Uparrow\uparrow\rangle$	$|\uparrow\uparrow\uparrow\rangle$
$5/2$	$|\Uparrow\uparrow\uparrow\rangle$	$|\downarrow\Uparrow\Uparrow\rangle$	0	0
$7/2$	$|\uparrow\Uparrow\Uparrow\rangle$	0	0	0
$9/2$	$|\Uparrow\Uparrow\Uparrow\rangle$	0	0	0

by application of the rotation operator C_3^j. These states are showed in Table I.

The corresponding states with all spins flipped, namely, with $M'=-M$, can be written in a similar form (not shown). Having identified the symmetric states in terms of the spin states, we proceed to analyze the allowed transitions induced in the spin systems by magnetic and electric field, both within the single valued group and double valued group representations.

1. Single valued group states of the $s=3/2$ triangle

The above states are basis of the point group D_{3h}, but not eigenstates of the total spin operator $\mathbf{S}^2$. The total spin eigenstates can be written as linear combinations of states with given M, S, and chirality (k): $|\psi_{S,M}^{(k)}\rangle=\Sigma_{l(M)}a_{k,l}^S|\psi_M^{(k,l)}\rangle$, where $l(M)$ is the number of different states with a given M. The coefficients $a_{k,l}$ are to be identified so that these states satisfy $\mathbf{S}^2|\psi_{S,M}^{(k)}\rangle=S(S+1)|\psi_{S,M}^{(k)}\rangle$, with $S=1/2,3/2,5/2,7/2,9/2$. The states with $k=0$ are all transforming according to the A_2' representation, while the states with $k=1,2$ are organized in doublets, being the bases of the two dimensional representation E'. The magnetic and electric transitions are similar to the ones in the $s=1/2$ triangle, in the absence of SOI. The electric field causes transitions only between states with the same M and S, but opposite chirality $C_z=(1/2\sqrt{3})\mathbf{s}_1\cdot(\mathbf{s}_2\times\mathbf{s}_3)$ (this is different from the triangle with $s_i=1/2$ spins in each of the vertices). As for the $s=1/2$ spin triangle, there are electric dipole transitions within the $S=1/2$ quadruplet, even in the absence of SOI. The ground state is fourfold degenerate consisting of two $S=1/2$ eigenstates,

$$|\psi_{M=1/2}^{(1)}\rangle = \frac{1}{\sqrt{10}}[|\psi_{M=1/2}^{(1,1)}\rangle + \sqrt{3}|\psi_{M=1/2}^{(1,2)}\rangle$$
$$- (\epsilon_1 - \epsilon_2)(|\psi_{M=1/2}^{(1,3)}\rangle - |\psi_{M=1/2}^{(1,4)}\rangle)], \qquad (18)$$

$$|\psi_{M=1/2}^{(2)}\rangle = \frac{1}{\sqrt{10}}[|\psi_{M=1/2}^{(2,1)}\rangle + \sqrt{3}|\psi_{M=1/2}^{(2,2)}\rangle$$
$$+ (\epsilon_1 - \epsilon_2)(|\psi_{M=1/2}^{(2,3)}\rangle - |\psi_{M=1/2}^{(2,4)}\rangle)]. \qquad (19)$$

As in the case of the $s=1/2$ triangle, electric-field induced transitions take place between the states of opposite chirality C_z and same spin projection M. Besides, the lowest quadruplet states are still organized as spin and chirality eigenstates that are split in the presence of SOI.

In the original spin Hamiltonian in Eq. (1) the electric field causes modification of the spin Hamiltonian parameters. As for the spin $s=1/2$ triangle, the strongest effect comes from modification of the isotropic exchange interaction so that

$$\delta H_0(\mathbf{E}) = \sum_{i=1}^{3} \delta J_{ii+1}(\mathbf{E})\mathbf{s}_i \cdot \mathbf{s}_{i+1}, \qquad (20)$$

with $\delta J_{ii+1}(\mathbf{E})=dE\cos(2\pi i/3+\theta)$, where θ is the angle between the projection of the external electric field $\mathbf{E}$ to the molecule's plane and the $\mathbf{s}_1-\mathbf{s}_2$ bond, and $i=0,1,2$. The effect of the electric field on the lowest quadruplet is found to be similar to the spin $s=1/2$ case. While the SOI splits the two chiral states without mixing them (at least in lowest order), the electric field, on the other hand, mixes the chiral states. The effective Hamiltonian acting in the lowest quadruplet reads

$$H_{\text{eff}} = \Delta_{\text{SO}}C_z S_z + \mathbf{B}\cdot\bar{\bar{g}}\mathbf{S} + d'\mathbf{E}\cdot\mathbf{C}_\parallel. \qquad (21)$$

Above, $d'=3d/2$, $\mathbf{C}_\parallel=(C_x,C_y,0)$, with $C_x=\Sigma_M|\psi_M^{(1)}\rangle\langle\psi_M^{(2)}|+|\psi_M^{(2)}\rangle\langle\psi_M^{(1)}|$ and $C_x=i\Sigma_M(|\psi_M^{(1)}\rangle\langle\psi_M^{(2)}|-|\psi_M^{(2)}\rangle\langle\psi_M^{(1)}|)$, and Δ_{SO} stands for the SO splitting. However, in this situation the in-plane chirality operators $C_{x,y}$ cannot be written in a simple form as a function of the individual spin operators, as opposed to the $s=1/2$ triangle.

2. Double valued group states of the $s=3/2$ triangle

The double group representation allows us to identify the couplings between different spin states induced by the SOI and to identify the allowed magnetic dipole transitions. Due to SOI, the electric field induced spin transitions will take place also outside the spin quadruplet. In the absence of extra degeneracies (induced, for example, by external magnetic fields), however, these transitions are strongly reduced due the gap of the order J. We can then focus, as for the $S=1/2$ triangle, only on the lowest quadruplet. These states are organized in two Kramer doublets $\bar{E}'$ and $\bar{E}''$ transforming as $M=\pm1/2$ and $M=\pm3/2$.

As in the case of the $s=1/2$ triangle, the electric field induced transitions take place between $\bar{E}'$ and $\bar{E}''$, with the selection rules $\Delta M=\pm2$. Magnetic transitions instead take place both within and between $\bar{E}'$ and $\bar{E}''$, satisfying the selection rules $\Delta M=0,\pm1$.

If we now treat the SOI, electric field, and magnetic fields on the same footing, we arrive at the same selection rules as for the $s=1/2$ triangle, namely, $\Delta C_z=\pm1$ and $\Delta S_z=0$ for electric transitions, $\Delta C_z=0,\pm1$ and $\Delta S_z=0,\pm1$ for SOI transitions, and $\Delta C_z=0$ and $\Delta S_z=0,\pm1$ for magnetic transitions, respectively.

C. Spin $s=1/2$ pentagon

We now analyze the spin-electric coupling in a pentagonal molecule with a spin $s=1/2$ in each of the vertices, like depicted schematically in Fig. 3. As in the case of the spin triangle, an external electric field $\mathbf{E}$ gives rise to modification of exchange couplings J_{ii+1}. However, the net spin-electric
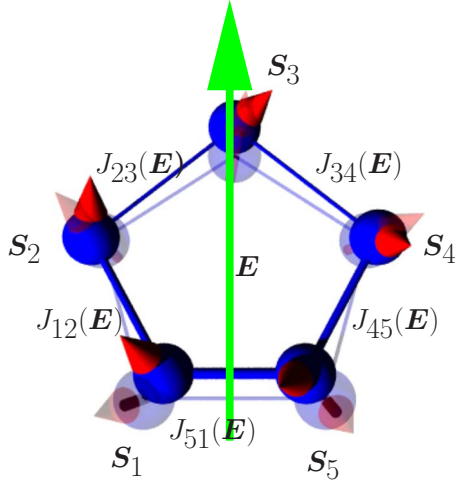
FIG. 3. (Color online) Schematics of a pentagonal spin ring molecule in electric field **E**, light (green) arrow. The molecule in the absence of electric field is depicted in fade colors, while the full colors represent the molecules in electric field. Thickness of the bonds represents the strength of antiferromagnetic exchange interaction between the spins. An electric field modifies the strengths of spin exchange couplings J_{ii+1}.

coupling in the lowest spin sector can only be mediated by SOI, i.e., via the DM interaction.

To make the analysis simpler, we assume in the following that the pentagonal spin molecule possesses a D_5 point group symmetry, thus no horizontal reflection plane σ_h. However, no generality is lost since lower symmetry implies more allowed transitions in the spin system. If, for example, in the lower symmetric situation some transitions are forbidden, these transitions will be also forbidden in the higher symmetry case. The Hamiltonian is given in Eq. (1) with $N=5$. The states of the pentagon are found from the product of the individual spin representations $D_{tot}=D^{(1/2)\otimes 5}=5D^{(1/2)}\oplus 4D^{(3/2)}\oplus D^{(5/2)}$, meaning there are 32 spin states in total. As before, these states can be organized in a symmetry adapted basis in the following way:

$$|\psi_M^{(k,i)}\rangle = P_5^k|M,i\rangle, \tag{22}$$

$$P_5^k = \frac{1}{\sqrt{5}}\sum_{j=0}^{4}\epsilon_j^k C_5^j, \tag{23}$$

where $\epsilon_j^k=\exp(2i\pi jk/5)$ with $k,j=0,\ldots,5$, C_5^j are the fivefold rotations of order j. The states $|M,i\rangle\equiv|\sigma_1\sigma_2\sigma_3\sigma_4\sigma_5\rangle$ represent all possible states (i states in total) with a given spin projection $M(\equiv\Sigma_k\sigma_k)$ that cannot be transformed into each other by application of the rotation operator C_5^j. These states are showed in Table II and the corresponding states with all spins flipped, i.e., $M\rightarrow -M$ states (not shown). In the absence of SOI there is no mixing of different k states, i.e. the chirality is a good quantum number. In this case the chirality is quantified by the operator $C_z = 1/(2\sqrt{5+2\sqrt{5}})\Sigma_i\mathbf{s}_i\cdot(\mathbf{s}_{i+1}\times\mathbf{s}_{i+2})$ (the prefactor is chosen for convenience; see below). The ground-state quadruplet consists of two Kramers doublets with spin $S=1/2$. In the fol-

TABLE II. Spin $s=1/2$ pentagon nonsymmetry adapted states.

M	i	
	1	2
1/2	$|\uparrow\downarrow\uparrow\downarrow\uparrow\rangle$	$|\uparrow\downarrow\downarrow\uparrow\uparrow\rangle$
3/2	$|\downarrow\uparrow\uparrow\uparrow\uparrow\rangle$	0
5/2	$|\uparrow\uparrow\uparrow\uparrow\uparrow\rangle$	0

lowing we inspect the level structure of these four states in terms of the above symmetry adapted states.

1. Single valued group $s=1/2$ pentagon

We focus here only on the four lowest energy states, which are two pairs of $S=1/2$ states. The first (second) pair is given by linear combination of states with $k=1(k=-1)$ and spin projection $M=\pm 1/2$. We obtain

$$|\psi_{S=1/2,M=\pm 1/2}^{(k)}\rangle = \frac{1}{\sqrt{3}}\left[\frac{1}{2\cos\left(\frac{2k\pi}{5}\right)}|\psi_{M=\pm 1/2}^{(k,1)}\rangle + 2\epsilon_2^k\cos\left(\frac{2\pi}{5}\right)|\psi_{M=\pm 1/2}^{(k,2)}\rangle\right], \tag{24}$$

so that $C_z|\psi_{M=\pm 1/2}^{(k)}\rangle=(-1)^k|\psi_{M=\pm 1/2}^{(k)}\rangle$. These states (for a given M projection) form the basis of the two-dimensional irreducible representation E_1. We are now in positions to investigate the allowed electric dipole transitions within this lowest subspace. The in-plane electric dipole $\mathbf{d}=(d_x,d_y)$ forms a basis of the irreducible representation E_1 in D_5.[49] By calculating the product $E_1\otimes E_1\otimes E_1=2E_1\oplus 2E_2$, with E_2 being another two-dimensional irreducible representation of D_5, we see that the totally symmetric representation A_1 of D_5 is absent. Therefore, there are *no* electric dipole transitions within the four-dimensional subspace in the absence of SOI.

As in the previous two cases, the coupling of the spin Hamiltonian to electric field comes via modification of the spin Hamiltonian parameters. If only the modification of the isotropic exchange Hamiltonian is taken into account, the spin-electric Hamiltonian takes the same form as in Eq. (7), with $\delta J_{ii+1}(\mathbf{E})=dE\cos(2i\pi/5+\theta)$, $i=1,\ldots,5$. The parameter d quantifies the electric dipole coupling of each of the bonds and θ is the angle between the electric field **E** and the bond $\mathbf{s}_1-\mathbf{s}_2$. Note that d is in principle non-zero in D_5 point group symmetry. However, the matrix elements of the spin-electric Hamiltonian within the lowest quadruplet are all zero, i.e., $\langle\psi_{S=1/2,M}^{(k)}|\delta H_{e-d}(\mathbf{E})|\psi_{S=1/2,M'}^{(k')}\rangle\equiv 0$. This means that electric field has no effect on the lowest quadruplet, as found out also by purely symmetry arguments. Therefore, we may expect that the spin-electric coupling in pentagonal spin molecule is caused by SO effects.

2. Double valued group $s=1/2$ pentagon

The lowest four states in the double group D_5' are described by the two dimensional irreducible representations

$\bar{E}_1'(M = \pm 1/2)$ and $\bar{E}_1''(M = \pm 3/2)$. Since both the magnetic μ and electric **d** dipoles transform as E_1 in D_5', both electric and magnetic transitions will take place between the same pair of states. The products of the irreducible representations that labels the states in the low-energy quadruplet read $\bar{E}_1' \otimes \bar{E}_2'' = E_1 \oplus E_2$, $\bar{E}_1' \otimes \bar{E}_1' = A_1 \oplus A_2 \oplus E_1$ and $\bar{E}_2' \otimes \bar{E}_2' = A_1 \oplus A_2 \oplus E_2$. These equalities imply the same selection rules in the lowest subspace as for the spin triangle case: $\Delta M = \pm 2$ for electric dipole transitions, and $\Delta M = 0, \pm 1$ for the magnetic ones.

The main feature of the pentagonal spin ring is the absence of electric dipole transitions in the lowest quadruplet in the absence of SOI. This is to be contrasted with the spin triangle case, where spin-electric coupling exists in the ground state even in the absence of SOI. This feature finds its explanation in the interplay between the selection rules for electric field transitions and the ones for the SOI. In fact, these selection rules are by no means different from the triangular spin rings. Since the ground state is spanned by four states with chirality $C_z = -1, 1$ and spin $S_z = \pm 1/2$, we see that the condition $\Delta C_z = \pm 1$ for the electric field transitions implies no electric field coupling within the ground state. In the presence of SOI though, spin electric coupling is still possible, but it will be $(D_{x,y}/J)$ times smaller than in triangles. Spin-electric coupling can arise also via modification of the DM vectors $D_{x,y,z}$ in electric field. However, the selection rules for this transitions are, like for the triangle, $\Delta C_z = 0, \pm 2$ and $\Delta S_z = 0, \pm 1$. This means direct splitting in the ground state, and thus we expect that for pentagonal spin rings the electric dipole response will be much weaker.

D. Symmetry requirements for the existence of spin-electric coupling

There are two general feature that allow for the manipulation of the MN state vector within the ground-state multiplet, through pulsed electric fields. (For simplicity, we refer to the case where such coupling is not mediated by spin-orbit interaction and appears in a triangular molecule.)

Firstly, in order for the spin-electric Hamiltonian to be linear in the electric field, permanent electric dipoles $\mathbf{d}_{ij}$ must be present on the bridge(s) that mediate the coupling of spins i and j. These dipole moments must depend on the relative orientation of $\mathbf{s}_i$ and $\mathbf{s}_j$, see Fig. 4. Besides, in order for the electric field to modify differently the super-exchange couplings J_{ij} between different pairs of spins, the dipoles $\mathbf{d}_{ij}$ must point in different directions from one another. In the present case (10), the $\mathbf{d}_{ij}$ are orthogonal to the vectors $\mathbf{R}_{ij}$, other in-plane components being forbidden by symmetry. If the dipoles associated with the spin pairs are all along the same direction, instead, the electric field can only induce equal renormalizations of all the exchange couplings ($\delta J_{ij} \equiv \delta J$). As a consequence, the spin-electric Hamiltonian δH_E would commute with H_0 and could not induce transitions between eigenstates of the unperturbed Hamiltonian. In a recent study of spin crossover effect,[53] the total molecular electric dipole moment was shown to cause influence the spin state of the molecule. In the mechanism considered here, we require only the existence of the bridge dipole mo-
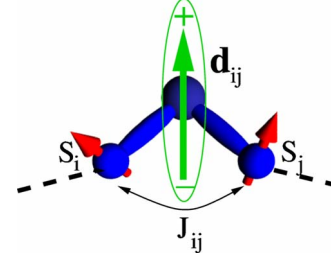

FIG. 4. (Color online) Dipole moment of an unperturbed bridge. In the first order, external electric fields couple to the electric dipole moments of the bridges that connect the spins at magnetic centers. The different orientations of the bridge dipole moments $\mathbf{d}_{ij} \neq \mathbf{d}_{kl}$ lead to inhomogeneous variations of the resulting exchange interactions between the spins $\delta J_{ij} \neq \delta J_{kl}$.

ment, while the total dipole moment of the molecule may be zero.

Secondly, given the existence of a spin-electric coupling, we require that this allows nontrivial manipulations of the MN quantum state within the low-energy multiplet. In particular, in the case of triangle, our proposal relies on the existence of a four-dimensional ground-state multiplet (with $S = 1/2$), whose states are identified by the spin projection $|S_z| = 1/2$ and by chirality C_z. This condition is fulfilled by rings consisting of an odd number of half integer and equivalent spins. Within these class of systems, triangles are particularly suited because the two eigenstates of chirality can be coupled in first order by the spin-electric Hamiltonian even in the absence of spin-orbit interaction.

Both the above criteria can be formulated in terms of inversion symmetry. As far as the first criterion is concerned, the superexchange bridges that magnetically couple $\mathbf{s}_i$ and $\mathbf{s}_j$ must lack an inversion center, though this condition is not sufficient in order for the bridge to possess a permanent electric dipole. Regarding the level structure and selection rules (second criterion), the presence of an odd number of equivalent spins in the ring implies the lack of an inversion center for the molecule as a whole.

III. HUBBARD MODEL OF A MOLECULAR NANOMAGNET

Spin Hamiltonian models of molecular nanomagnets are based on the assumption that the spins on magnetic centers are the only relevant degrees of freedom. This assumption of fully quenched and localized orbitals allows for the relatively simple predictions of spin structure in the low-energy states of the molecule. However, since the orbital dynamics plays a crucial role in the spin-electric coupling, spin Hamiltonian models are unable to predict the corresponding coupling constants. In this section, we relax the assumption of quenched and localized orbitals and treat the orbital degrees of freedom of electrons on magnetic ions within a Hubbard model. This provides an intuitive picture of spin-electric coupling in terms of the deformation of the molecular orbitals induced by the external field. Besides, in the limit of strong quenching of the orbitals, the Hubbard model reproduces a spin Hamiltonian, similar to the results found in the studies of

cuprates[54–56] and multiferroics.[57,58] In particular, we find the relation between modifications of the electronic hopping matrix elements induced by the field and that of the spin-electric coupling in the spin Hamiltonian, thus providing a guide for the estimate of the size of spin-electric coupling in a molecule.

The outline of the present section is the following. In Sec. III A, we introduce the Hubbard model of a spin chain with the shape of regular n-tangon and derive the resulting symmetry constraints for the hopping parameters. In Sec. III B we assume a direct electron hopping between magnetic sites and derive the spin Hamiltonian of a spin triangle from the Hubbard model in the limit of large on-site repulsions; we thus express the coupling to electric fields in terms of the Hubbard model parameters. In Sec. III C, we introduce a Hubbard model of a magnetic coupling in the case where this is mediated by a nonmagnetic bridge between the magnetic centers; also in this case, we find a connection between the modification of the bridge and spin-electric coupling.

A. Parameters of the Hubbard model of molecular nanomagnets

Magnetic properties of molecular nanomagnets are governed by the spin state of few electrons in the highest partially occupied atomic orbitals, split by the molecular field. The spin density is localized on the magnetic centers,[59] and thus the low-energy magnetic properties are correctly described by quantum models of interacting localized spins.[60,61]

The response of molecular nanomagnets to electric fields, as a matter of principle, does not have to be governed by the electrons occupying the same orbitals that determine the molecule's spin. However, the quantum control of single molecule magnets by electric fields depends on the electrons that both react to electric fields and produce the magnetic response. Therefore, the models of molecular nanomagnets that consider only few orbitals can provide useful information about the electric control of spins.

Hubbard model provides a simplified description of orbital degrees of freedom by including only one or few localized orbitals on each magnetic center. Furthermore, the interaction between electrons is accounted for only by introducing the energies of the atomic configurations with different occupation numbers. The Hubbard model of the MN is given by

$$H_\mathrm{H} = \left[\sum_{i,j} \sum_{\alpha,\beta} c_{i\alpha}^\dagger \left(t\delta_{\alpha\beta} + \frac{i\mathbf{P}_{ij}}{2} \cdot \boldsymbol{\sigma}_{\alpha\beta} \right) c_{j\beta} + \mathrm{H.c.} \right] + \sum_j U_j(n_{j\uparrow}, n_{j\downarrow}), \quad (25)$$

where $c_{j\sigma}^\dagger$($c_{j\sigma}$) creates (annihilates) an electron with spin $\sigma = \uparrow, \downarrow$ on the orbital localized on jth atom, and $n_{j\sigma} = c_{j\sigma}^\dagger c_{j\sigma}$ is the corresponding number operator. Model parameters U_j describe the energy of $n_{j\uparrow(\downarrow)}$ spin up(down) electrons on the site j. Hopping parameters t_{ij} and $\mathbf{P}_{ij}$ describe the spin-independent and spin-dependent hopping between sites i and j.

We assume that the largest energy scale is the splitting between the energy of the highest occupied atomic orbital and lowest unoccupied one, induced by the molecular crystal field: this justifies the inclusion of one orbital only for each magnetic center. The on-site repulsion energy is the next largest energy scale in the problem, being U_j larger than the hopping coefficients. Among these, processes involving states of different spin, mediated by spin-orbit interaction, are described by the x and y components of $\mathbf{P}_{ij}$. The parameters $P_{ij;z}$, instead, describe the difference of the hopping matrix elements between spin-up and spin-down electrons. In the following, we shall consider both the case where electron hopping takes place directly between neighboring magnetic ions and that where the magnetic interaction is mediated by bridges of nonmagnetic atoms. Hubbard model with spin-dependent hopping was used to describe the spin-orbit coupling in cuprates[62] and multiferroics.[57] The Hubbard Hamiltonian can be approximated by a spin Hamiltonian model in the limit $|t_{ij}|, |\mathbf{P}_{ij}| \ll U_j$. The symmetry constraints on the spin Hamiltonian parameters can be deduced from those on the Hubbard model parameters.[54] If the spin-independent hopping dominates ($|t| \gg |\mathbf{P}|$), the resulting spin Hamiltonian will contain the Heisenberg exchange terms and a small additional spin-anisotropic interaction. If $|t| \gtrsim |\mathbf{P}|$, the size of spin-dependent interactions in the spin Hamiltonian will be comparable to the Heisenberg terms. Both these cases appear in the molecule nanomagnets.[18,51,63,64]

Symmetry of the molecule imposes constraints to the Hubbard model, thus reducing the number of free parameters. The on-site repulsion parameters U_j are equal for all equivalent magnetic ions. In the molecules of the form of regular n-tagon, all of the spin-independent hopping parameters are equal due to the C_n symmetry. The spin-dependent hopping elements are related by both the full symmetry of the molecule and the local symmetry of localized orbitals. For example, in the case of localized orbitals in a regular polygon that are invariant under the local symmetry group of the magnetic center,

$$P_{j,j+1;x} = \exp\left[i\frac{2\pi(j-k)}{n} \right] P_{k,k+1;x}, \quad (26)$$

with the convention that site $n+1$ coincides with site 1. In this case, there is only one free parameter that determines all of the P_x matrix elements. Therefore, the regular n–tagon molecule in the absence of external electric and magnetic fields can be described by a Hubbard model, with five independent parameters: U, t, and $\mathbf{P}_{12}$. In addition, the σ_v symmetry, if present will impose $\mathbf{P}_{12} = p\mathbf{e}_z$, thus reducing the number of free parameters to three.

B. Hubbard model of the spin triangle: Direct exchange

In this section we give a brief description of the Hubbard model for a triangular molecule with D_{3h} symmetry. In this model we assume only direct coupling between the magnetic centers, thus no bridge in-between. Even so, this simplified model catches the main features of the effective spin Hamiltonian and gives the microscopic mechanisms for the spin-electric coupling. The Hamiltonian describing the electrons in the triangular molecule reads

$$H_H = \left[\sum_{i,\sigma} c_{i\sigma}^\dagger (t + i\sigma\lambda_{SO}) c_{i+1,\sigma} + \text{H.c.} \right]$$
$$+ \sum_{i,\sigma} \left(\epsilon_0 n_{i\sigma} + \frac{1}{2} U n_{i\sigma} n_{i\bar{\sigma}} \right), \tag{27}$$

where $\lambda_{SO} \equiv p = \mathbf{P}_{ij} \cdot \mathbf{e}_z$ is the spin-orbit parameter (only one), ϵ_0 is the on-site orbital energy, and U is the on-site Coulomb repulsion energy. As stated before, typically $\lambda_{SO}, |t| \ll U$, which allows for a perturbative treatment of the hopping and spin-orbit Hamiltonians. These assumptions agree well with the numerical calculations performed in Ref. 59.

The perturbation theory program involves the unperturbed states of the system. The first set of unperturbed states are the one-electron states

$$|\phi_i^\sigma\rangle = c_{i\sigma}^\dagger |0\rangle, \tag{28}$$

while the three-electron states split in two categories: (i) the singly occupied site states

$$|\psi_k^\sigma\rangle = \prod_{j=1}^3 c_{j\sigma_j}^\dagger |0\rangle, \tag{29}$$

with $\sigma_j = \sigma$ for $j \neq k$ and $\sigma_j = \bar{\sigma}$, for $j = k$, and (ii) the double-occupied sites

$$|\psi_{kp}^\sigma\rangle = c_{k\uparrow}^\dagger c_{k\downarrow}^\dagger c_{p\sigma}^\dagger |0\rangle, \tag{30}$$

with $k = 1, 2, 3$ and $p \neq k$. The states $|\psi_k^\sigma\rangle$ and $|\psi_{kp}^\sigma\rangle$ span the subspaces with $M = 1/2$ and $M = -1/2$ for $\sigma = \uparrow$ and $\sigma = \downarrow$, respectively.

The states in Eqs. (28)–(30) are degenerate with energies $E = \epsilon_0$, $E = 3\epsilon_0$, and $E = 3\epsilon_0 + U$, respectively. Note that these state are eigenstates of the Hamiltonian in Eq. (27) only in the absence of tunneling and SOI.

The above defined states are not yet adapted to the symmetry of the system, i.e., they are not basis states of the corresponding irreducible representations of D_{3h} point group. Finding these states is required by the fact that the symmetry of the molecule is made visible through the hopping and SOI terms in the Hubbard Hamiltonian. This is accomplished by using the projector operator formalism.[49] We obtain for the one-electron symmetry adapted states.

$$|\phi_{A_1'}^\sigma\rangle = \frac{1}{\sqrt{3}} \sum_{i=1}^3 |\phi_i^\sigma\rangle, \tag{31}$$

$$|\phi_{E_\pm'}^\sigma\rangle = \frac{1}{\sqrt{3}} \sum_{i=1}^3 \epsilon_{1,2}^{i-1} |\phi_i^\sigma\rangle, \tag{32}$$

where A_2' and $E_\pm'$ are one-dimensional and two-dimensional irreducible representations in D_{3h}, respectively. Similarly, the symmetry adapted states with the singly-occupied magnetic centers read

$$|\psi_{A_2'}^{1\sigma}\rangle = \frac{1}{\sqrt{3}} \sum_{i=1}^3 |\psi_i^\sigma\rangle, \tag{33}$$

$$|\psi_{E_\pm'}^{1\sigma}\rangle = \frac{1}{\sqrt{3}} \sum_{i=1}^3 \epsilon_{1,2}^{i-1} |\psi_i^\sigma\rangle, \tag{34}$$

while the symmetry adapted states of the doubly-occupied magnetic centers read

$$|\psi_{A_{1,2}'}^{2\sigma}\rangle = \frac{1}{\sqrt{6}} \sum_{i=1}^3 (|\psi_{i1}^\sigma\rangle \pm |\psi_{i2}^\sigma\rangle), \tag{35}$$

$$|\psi_{E_\pm'1}^{2\sigma}\rangle = \frac{1}{\sqrt{6}} \sum_{i=1}^3 \epsilon_{1,2}^{i-1} (|\psi_{i1}^\sigma\rangle + |\psi_{i2}^\sigma\rangle), \tag{36}$$

$$|\psi_{E_\pm'2}^{2\sigma}\rangle = \frac{1}{\sqrt{6}} \sum_{i=1}^3 \epsilon_{1,2}^{i-1} (|\psi_{i1}^\sigma\rangle - |\psi_{i2}^\sigma\rangle). \tag{37}$$

The tunneling and SOI mixes the singly-occupied and doubly-occupied states. Since both the tunneling and SOI terms in the Hubbard Hamiltonian transform as the totally symmetric irreducible representation A_1' in D_{3h}, only states transforming according to the same irreducible representations Γ mix. We obtain the perturbed states in first order in t/U and λ_{SO},

$$|\Phi_{A_2'}^{1\sigma}\rangle \equiv |\psi_{A_2'}^{1\sigma}\rangle, \tag{38}$$

$$|\Phi_{E_\pm'}^{1\sigma}\rangle \equiv |\psi_{E_\pm'}^{1\sigma}\rangle + \frac{(\bar{\epsilon}-1)(t \pm \sigma\lambda_{SO})}{\sqrt{2}U} |\psi_{E_\pm'1}^{2\sigma}\rangle,$$

$$+ \frac{3\epsilon(t \pm \sigma\lambda_{SO})}{\sqrt{2}U} |\psi_{E_\pm'2}^{2\sigma}\rangle. \tag{39}$$

Doubly-occupied states become high in energy when $|t|/U, \lambda_{SO}/U \ll 1$. In this limit, the orbital states are quenched into singly-occupied localized atomic orbitals, and low-energy behavior is determined by spin and described by a spin Hamiltonian. In this limit the states in Eq. (34) are exactly the same chiral states in the spin Hamiltonian, i.e., $|\psi_{E_\pm'}^{1\sigma}\rangle \equiv |\psi_\sigma^{(1,2)}\rangle$ and $|\psi_{A_2'}^{1\sigma}\rangle \equiv |\psi_\sigma^{(0)}\rangle$. The probability of finding two electrons at the same site decays as $|t|/U$. The lowest energy states have total spin $S = 1/2$ and the chirality $C_z = \pm 1$, and the fluctuations of chirality $\Delta C_z = \sqrt{\langle C_z^2\rangle - \langle C_z\rangle^2}$ in the eigenstates vanish, see Fig. 5. The chiral states emerge as the eigenstates in the large-U limit, when the system is well described by the spin Hamiltonian:

The coupling of the molecule to an external electric field $\mathbf{E}$ takes place via two mechanisms. The first one implies modification of the on-site single particle energies ϵ_0 and leads to the following electric-dipole coupling Hamiltonian:

$$H_{e-d}^0 = -e \sum_\sigma \frac{E_y a}{\sqrt{3}} c_{1\sigma}^\dagger c_{1\sigma} - \frac{a}{2} \left(\frac{E_y}{\sqrt{3}} + E_x \right) c_{2\sigma}^\dagger c_{2\sigma}$$
$$+ \frac{a}{2} \left(E_x - \frac{E_y}{\sqrt{3}} \right) c_{3\sigma}^\dagger c_{3\sigma}, \tag{40}$$

with a being the geometrical distance between the magnetic ions and $E_{x,y}$ the in-plane components of the electric field.
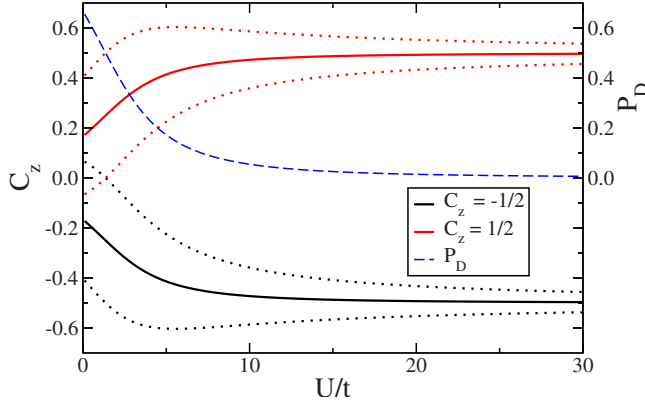
FIG. 5. (Color online) Spin Hamiltonian limit. Expectation values of chirality $\langle C_z \rangle$ (full lines) and the their bounds of uncertainty $\langle C_z \rangle \pm \Delta C_z$ (dotted lines), see text, in the low-energy states of the Hubbard model as a function of the on-site repulsion U at the fixed hopping matrix element $t=1$ (left scale). The dashed line shows dependence of the double occupancy probability P_D in the ground state on the right scale. The spin Hamiltonian description becomes accurate in the $U \rightarrow \infty$ limit. The approach to this limit is slow, and the double occupancy probability is proportional to t/U.

The second mechanism is due to modification of the hopping parameters t_{ii+1} in electric field and gives

$$H^1_{\text{e-d}} = \sum_{i,\sigma} t^{\mathbf{E}}_{ii+1} c^{\dagger}_{i\sigma} c_{i+1\sigma} + \text{H.c.}, \tag{41}$$

where $t^{\mathbf{E}}_{ii+1} = \langle \phi_{i\sigma} | -e\mathbf{r} \cdot \mathbf{E} | \phi_{i+1\sigma} \rangle$ are new hopping parameters induced solely by the electric field $\mathbf{E}$, and $\Phi_{i\sigma}$ are the Wannier states localized on the magnetic centers. We can write the $\mathbf{E}$-induced hoppings as $t^{\mathbf{E}}_{ii+1} = \Sigma_{q=x,y,z} q_{ii+1} E_q$, with $q_{ii+1} = -\langle \phi_{i\sigma} | eq | \phi_{i+1\sigma} \rangle$ being electric dipole matrix elements between the i and $i+1$ ions. These matrix elements are not all independent, symmetry alone reducing drastically the number of independent electric dipole parameters. In order to find suitable independent free parameters, we switch from the description in terms of localized Wannier orbitals $\Phi_{i\sigma}$, to the description in terms of symmetry adapted states, namely from q_{ii+1} to $q_{\Gamma\Gamma'} = \langle \phi_{\Gamma\sigma} | q | \phi_{\Gamma'\sigma} \rangle$, where $\Gamma = A'_1, E'_{\pm}$. In the basis of symmetry adapted states, the components $q_{\Gamma\Gamma'}$ satisfy a number of relations. In particular, we find

$$\langle \phi^{\sigma}_{A'_1} | x | \phi^{\sigma}_{A'_1} \rangle = \langle \phi^{\sigma}_{A'_1} | y | \phi^{\sigma}_{A'_1} \rangle = \langle \phi^{\sigma}_{E'_+} | x | \phi^{\sigma}_{E'_+} \rangle \equiv 0, \tag{42}$$

$$\langle \phi^{\sigma}_{E'_-} | x | \phi^{\sigma}_{E'_-} \rangle = \langle \phi^{\sigma}_{E'_+} | y | \phi^{\sigma}_{E'_+} \rangle = \langle \phi^{\sigma}_{E'_-} | y | \phi^{\sigma}_{E'_-} \rangle \equiv 0, \tag{43}$$

$$\langle \phi^{\sigma}_{E'_+} | x | \phi^{\sigma}_{E'_-} \rangle = -i \langle \phi^{\sigma}_{E'_+} | y | \phi^{\sigma}_{E'_-} \rangle \equiv -d_{EE}/e, \tag{44}$$

$$\langle \phi^{\sigma}_{A'_1} | x | \phi^{\sigma}_{E'_+} \rangle = \langle \phi^{\sigma}_{A'_1} | x | \phi^{\sigma}_{E'_-} \rangle = -i \langle \phi^{\sigma}_{A'_1} | y | \phi^{\sigma}_{E'_+} \rangle = i \langle \phi^{\sigma}_{A'_1} | y | \phi^{\sigma}_{E'_-} \rangle$$
$$\equiv -d_{AE}/e. \tag{45}$$

These relations reduce the number of free coupling constants to two, namely, d_{EE} and d_{AE}.

It is instructive to write first the relation between the second quantized operators $c^{\dagger}_{i\sigma}(c_{i\sigma})$ and $c^{\dagger}_{\Gamma\sigma}(c_{\Gamma\sigma})$, which create

(annihilate) electrons in localized and symmetry adapted states, respectively,

$$\begin{pmatrix} c^{\dagger}_{1\sigma} \\ c^{\dagger}_{2\sigma} \\ c^{\dagger}_{2\sigma} \end{pmatrix} = \frac{1}{\sqrt{3}} \begin{pmatrix} 1 & 1 & \epsilon \\ 1 & \bar{\epsilon} & \bar{\epsilon} \\ 1 & \epsilon & 1 \end{pmatrix} \begin{pmatrix} c^{\dagger}_{A'_1\sigma} \\ c^{\dagger}_{E'_+\sigma} \\ c^{\dagger}_{E'_-\sigma} \end{pmatrix}. \tag{46}$$

With these expressions at hand, we can write the electric dipole Hamiltonian together with the spin-orbit Hamiltonian in the following form:

$$H^0_{\text{e-d}} = \frac{-iea\sqrt{3}}{2} \sum_{\sigma} (\bar{E} c^{\dagger}_{E'_+\sigma} c_{A'_1\sigma} - \epsilon E c^{\dagger}_{E'_-\sigma} c_{A'_1\sigma} + \epsilon \bar{E} c^{\dagger}_{E'_-\sigma} c_{E'_+\sigma})$$
$$+ \text{H.c.}, \tag{47}$$

$$H^1_{\text{e-d}} = \sum_{\sigma} d_{AE} (\bar{E} c^{\dagger}_{A'_1\sigma} c_{E'_+\sigma} - E c^{\dagger}_{A'_1\sigma} c_{E'_-\sigma}) + \bar{E} d_{EE} c^{\dagger}_{E'_+\sigma} c_{E'_-\sigma}$$
$$+ \text{H.c.}, \tag{48}$$

$$H_{\text{SO}} = \sqrt{3} \lambda_{\text{SO}} \sum_{\sigma} \sigma (c^{\dagger}_{E'_-\sigma} c_{E'_-\sigma} - c^{\dagger}_{E'_+\bar{\sigma}} c_{E'_+\bar{\sigma}}), \tag{49}$$

where $E = E_x + iE_y (\bar{E} = E_x - iE_y)$. The symmetry adapted states can also be expressed in terms of the symmetry adapted operators $c^{\dagger}_{\Gamma}$. The expressions for these states are shown in Appendix A. Using these states, we can compute all the matrix elements corresponding to the electric dipole and SOI Hamiltonian, respectively. The explicit form of these matrix elements can be found in Appendix B.

We now compute the electric dipole matrix elements between the perturbed chiral states of the $E_{\pm}$ symmetry. The question is to what order in t/U and/or $eEa(d_{EE}, d_{AE})/U$ we want to do it. We use the relations $|ea| \gg d_{EE}, d_{AE}$, which hold in the case of localized orbitals. This leads us to the following matrix element of the electric dipole in the ground state:

$$|\langle \Phi^{1\sigma}_{E'_-} | H^0_{\text{e-d}} | \Phi^{1\sigma}_{E'_+} \rangle| \propto \left| \frac{t^3}{U^3} eEa \right|, \tag{50}$$

$$|\langle \Phi^{1\sigma}_{E'_-} | H^1_{\text{e-d}} | \Phi^{1\sigma}_{E'_+} \rangle| \simeq \left| \frac{4t}{U} E d_{EE} \right|. \tag{51}$$

We now relate the SOI matrix elements to the DM vectors in the effective spin Hamiltonian. From Eq. (49) we get

$$\langle \Phi^{1\sigma}_{E'_\pm} | H_{\text{SO}} | \Phi^{1\sigma}_{E'_\pm} \rangle = \pm \frac{5\sqrt{3}\lambda_{\text{SO}} t}{2U} \text{sgn}(\sigma), \tag{52}$$

In the same time, in D_{3h} symmetry, the DM term reads

$$H_{\text{SO}} = \frac{iD_z}{2} \sum_{i=1}^{3} (s^i_+ s^{i+1}_- - s^i_- s^{i+1}_+), \tag{53}$$

allowing us to make the following identification:

$$D_z \equiv \frac{5\lambda_{SO}t}{U}. \tag{54}$$

We see that this SOI term acts exactly as the "microscopic" SOI derived before: it splits the chiral states, but it does not mix them.

The Hubbard model with spin-orbit coupling can reproduce the energy-level structure of the spin Hamiltonian. In the limit of strong on-site repulsion $|t|/U \ll 1$, the atomic orbitals in the triangle vertices are occupied by one electron each. The lowest energy manifold consists of four states with the total spin $S = 1/2$. These states are split from the next four-level $S = 3/2$ manifold by a gap of the order of t^2/U.

C. Superexchange in molecular bonds

In this section, we use the Hubbard model to deduce the dependence of the spin Hamiltonian of MNs on the external electric fields in the case where the coupling between magnetic sites is mediated by a nonmagnetic bridge. In particular, we study how the parameters of the effective spin Hamiltonian depend on the hopping matrix elements that are modified by the presence of an electric field. The spins in molecular nanomagnets are localized at the magnetic centers and interact through the long bridges of nonmagnetic atoms. In addition, we do not expect that these orbitals deform in the electric field. Therefore, we expect that the superexchange mechanism through the bridge is more significant than the direct exchange. This method was successfully applied in the studies of strongly correlated electrons, like cuprates[56] and multiferroics.[58]

In order to describe the magnetic coupling, we consider a pair of sites corresponding to the magnetic centers and a bridge site. Since the direct overlap of the orbitals localized on the magnetic centers is small, we set the direct hopping between the magnetic centers to zero but allow for the hopping of electrons between the magnetic sites and the bridge site. This hopping gives rise to superexchange interaction between the spins on the magnetic sites.[54] In the limit of strong on-site repulsions, the effective Hamiltonian in the lowest energy sector of the bond corresponds to a spin Hamiltonian where the coupling strengths are determined by the Hubbard model parameters. This correspondence provides an intuitive picture of the mechanism that leads to the interaction between the spins. It also allows us to infer the properties of the molecule that lead to a strong spin-electric coupling, e.g., the delocalization of the orbitals and their local symmetry.

The Hubbard Hamiltonian of the bond is given by

$$H_b = \sum_{i,\alpha\beta} \left[c_{i\alpha}^\dagger \left(t_i \delta_{\alpha\beta} + \frac{i\mathbf{P}_i}{2} \cdot \boldsymbol{\sigma}_{\alpha\beta} \right) b_\beta + \text{H.c.} \right]$$
$$+ U_1(n_1) + U_2(n_2) + U_b(n_b), \tag{55}$$

where the indices 1 and 2 refer to the magnetic sites, and b refers to the bridge site. We derive the spin Hamiltonian by fourth-order Schrieffer-Wolff transformation of the Hamiltonian H_b.

The Schrieffer-Wolf transformation[65] of the bond Hamiltonian $H_b = H_0 + H_{tun}$, where the unperturbed Hamiltonian

$H_0 = U_1(n_1) + U_2(n_2) + U_b(n_b)$ produces an effective low energy Hamiltonian H_{12} that approximately describes the low-energy dynamics of the bond. The effective Hamiltonian is

$$H_{12} = \mathcal{P}e^S H_b e^{-S}\mathcal{P}, \tag{56}$$

where the antiunitary operator S is chosen so that the low-energy space of H_0 is decoupled from the high-energy space. This operator is found iteratively, $S = S^{(1)} + S^{(2)} + \cdots$ so that the nth order transformation $S^{(n)}$ removes the terms that couple the low- and high-energy states up to order n. The projector $\mathcal{P}$ projects to the low-energy states. In our system, the lowest order Schrieffer-Wolff transformation that gives a nontrivial contribution to the low-energy spin Hamiltonian is of fourth order, and the operator S is approximated as $S \approx \Sigma_{n=1}^4 S^{(n)}$.

The unperturbed Hamiltonian, $H_0 = U_1 + U_2 + U_b$, describes localized electrons, and the hopping H_{tun} acts as perturbation. The low-energy subspace of the unperturbed Hamiltonian is spanned by the states in which the magnetic ions are singly occupied, and the bridge is doubly occupied. The lowest-order terms that give rise to a nontrivial spin Hamiltonian, in the limit $|t|, |\mathbf{P}| \ll U$, are of the fourth order in t and $\mathbf{P}$.

The resulting interaction of the spins includes an isotropic exchange of strength J, a Dzyalozhinsky-Moriya interaction described by a vector $\mathbf{D}$, and an anisotropic exchange term described by a second rank symmetric traceless tensor $\boldsymbol{\Gamma}$,[66]

$$H_{12} = J\mathbf{S}_1 \cdot \mathbf{S}_2 + \mathbf{D} \cdot (\mathbf{S}_1 \times \mathbf{S}_2) + \mathbf{S}_1 \cdot \boldsymbol{\Gamma}\mathbf{S}_2. \tag{57}$$

Quite generally the interaction between two spins up to second order in $\mathbf{P}_{12}$ can be represented as an isotropic exchange of rotated spins.[56] However, since the frustration in the triangle is strong, it is a good approximation to take only the Dzyalozhinsky-Moriya interaction into account for the weak spin-orbit coupling, $|\mathbf{P}_{12}| \ll |t_{12}|$ when describing a full molecule.

In a bond with a single bridge site, the largest possible symmetry is C_{2v}. We introduce Cartesian coordinates with the x axis pointing from the magnetic center 1 to 2, y axis lying in the bond plane and pointing toward the bridge site, and the z axis normal to the bond plane (Fig. 6). The elements of the C_{2v} symmetry group are then rotation $R_{y,\pi}$ by π about the y axis, reflection σ_v in the yz plane, and reflection σ_h in the xy plane. Each of these symmetry operations imposes constraints on the parameters of H_b. In the case of localized orbitals that remain invariant under the local symmetries of their respective sites, the constraints resulting from the $R_{y,\pi}$ symmetry are

$$t_1 = t_2, \tag{58}$$

$$P_{x,1} = -P_{x,2}, \tag{59}$$

$$P_{y,1} = P_{y,2}, \tag{60}$$

$$P_{z,1} = -P_{z,2}. \tag{61}$$

The σ_v symmetry implies

$$t_1 = t_2, \tag{62}$$
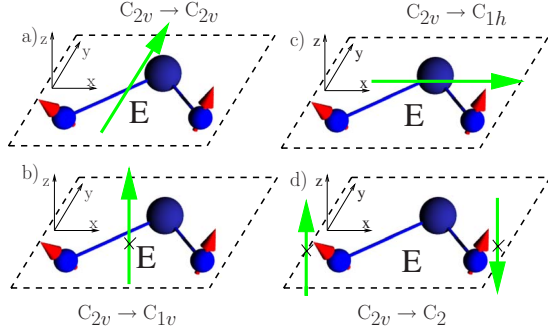
$$P_{x,1} = P_{x,2}, \tag{63}$$

FIG. 6. (Color online) Geometry of the bond and reduction of symmetry. (a) Electric field $\mathbf{E}$ in the y direction, leaves the C_{2v} symmetry unbroken. (b) An electric field $\mathbf{E}$ in the z direction, normal to the bond plane, reduces the symmetry to $\{E, \sigma_v\}$. (c) An electric field $\mathbf{E}$ in the x direction, along the line connecting the magnetic centers, reduces the symmetry to $\{E, \sigma_h\}$. (d) In an inhomogeneous staggered electric field $\mathbf{E}$, the reduced symmetry group is $\{E, R_{y,\pi}\}$.

$$P_{y,1} = -P_{y,2}, \tag{64}$$

$$P_{z,1} = -P_{z,2}, \tag{65}$$

and the σ_h symmetry implies

$$\mathbf{P}_1 = -\mathbf{P}_2 = p\mathbf{e}_z. \tag{66}$$

In the perturbative calculation of the effective spin Hamiltonian parameters, these constraints reproduce the Dzyalozhinsky-Moriya rules. We do not deal with the symmetry of on-site energies $U_{1,2,b}$ in any detail since they do not affect the spin Hamiltonian at this level of approximation.

D. Electric field along y

In the electric field pointing along the y axis, the point group symmetry of the bridge remains C_{2v}, and all of the constraints (59)–(66) hold. The fourth-order Schrieffer-Wolff transformation then gives the interaction between the spins on magnetic centers of form (57) with the parameters

$$J = \frac{1}{12U^3}(48t^4 - 40t^2p_z^2 + 3p_z^4), \tag{67}$$

$$\mathbf{D} = \frac{2}{U^3}tp_z(4t^2 - p_z^2)\mathbf{e}_z, \tag{68}$$

$$\Gamma_{xx} = \Gamma_{yy} = -\frac{1}{2}\Gamma_{zz} = -\frac{8}{3U^3}t^2p_z^2, \tag{69}$$

while all the off-diagonal elements of $\mathbf{\Gamma}$ vanish. Here, the parameters of the Hubbard model satisfy the symmetry constraints of the full C_{2v}, and

$$t_1 = t_2 = t, \tag{70}$$

$$\mathbf{P}_1 = -\mathbf{P}_2 = p_z\mathbf{e}_z. \tag{71}$$

We have introduced $U^3 = U_{c2}(2U_{c2} - U_{b2})(U_{b1} - U_{b2} + U_{c2})^2/(4U_{c2} - U_{b2})$, where the on-site repulsions are U_{b2} for

the doubly occupied bridge, U_{b1} for the singly occupied bridge, and U_{c2} for the doubly occupied magnetic center. The parameter U describes the energy cost of leaving the manifold of states with the minimal energy of Coulomb repulsion. We assume that the lowest energy charge configuration corresponds to a doubly occupied bridge, so that $U_{b2} < U_{b1}$.

In first order, the variations in the spin-Hamiltonian parameters resulting from the modification of the Hubbard model parameters are

$$\delta J = \frac{1}{3U^3}[(48t^3 - 20tp_z^2)\delta t + (-20t^2p_z + 3p_z^3)\delta p_z], \tag{72}$$

$$\delta D_z = \frac{2}{U^3}[(12t^2p_z - p_z^3)\delta t + (4t^3 - 3tp_z^2)\delta p_z], \tag{73}$$

$$\delta\Gamma_{xx} = \delta\Gamma_{yy} = -\frac{\delta\Gamma_{zz}}{2} = -\frac{16tp_z}{3U^3}(p_z\delta t + t\delta p_z). \tag{74}$$

Electric field modifies the orbitals and therefore the overlaps between them that determine the hopping parameters. We consider the case where the variations δt and δp_z are linear in the field intensity E_y: $\delta t = \kappa_t E_y$, $\delta p_z = \kappa_{p_z} E_y$. We will not discuss the effect of variations in the on-site energies U in any details since their only effect in the fourth-order perturbation is a rescaling of all the spin Hamiltonian parameters by $U^3/(U + \delta U)^3$.

We stress that these linear modifications of the hopping parameters are characteristic for the C_{2v} symmetry. If the electric field is oriented differently and thus lowers the system symmetry (see below) first-order increments are not allowed, and the spin-electric coupling is at least a second-order effect in the electric field. The modification of the orbitals includes the energy scale of splitting of the atomic orbitals in the molecular field. We have assumed earlier that the splitting of the orbitals localized on the magnetic centers is large, and the dominant source of the spin-electric coupling is the modification of the bridge orbital. Therefore, the key criterion for strong spin-electric coupling is the presence of bridge orbitals that are weakly split in the molecular field. If, in addition, we assume that the modification is a property of the bond alone, and not of the entire molecule, the κ parameters can be determined in an *ab initio* calculations on a smaller collection of atoms.

In the limit of weak spin-orbit coupling, $|t| \gg |p_z|$, the main effect of the electric fields is a change of J, leading to our symmetry-based results, see Eq. (15). In particular, the d parameter of the symmetry analysis is

$$d = \frac{4}{U^3}[(48t^3 - 20tp_z^2)\kappa_t + (-20t^2p_z + 3p_z^3)\kappa_{pz}]. \tag{75}$$

In this case, the Dzyalozhinsky-Moriya vector $\mathbf{D}$ is constrained to point in the z direction, $\mathbf{D} = D\mathbf{e}_z$. The model suggests that the dominant effect of the electric field in the molecules with dominant Heisenberg exchange ($J \gg |\mathbf{D}|$) is modification of the isotropic exchange constants J, and

$$\frac{|\delta \mathbf{D}|}{|\delta J|} \sim \frac{|\mathbf{D}|}{|J|}, \tag{76}$$

so that the modification of the Dzyalozhinsky-Moriya vector $\mathbf{D} \rightarrow \mathbf{D} + \delta \mathbf{D}$ is weaker. However, in the molecules in which the modifications of J are inefficient in inducing the spin-electric coupling, as, for example, in the spin-1/2 pentagon, the modifications of $\mathbf{D}$ may eventually provide the main contribution to the spin-electric coupling.

Electric field pointing in a generic direction breaks the C_{2v} symmetry of the bridge and allows further modification of the Hubbard and spin Hamiltonian parameters that do not obey all the symmetry constraints in Eqs. (58)–(66). With the relaxed constraints, both the direction and intensity of $\mathbf{P}_{1,2}$, as well as the spin-independent hoppings $t_{1,2}$ become field dependent. This observation can be used in the search for molecules that show strong spin-electric coupling. The energy cost of changing the distance between the localized orbitals may be significantly higher than the cost of modifying the shape of the bridge orbital. In order to investigate this dependence, we study the effective spin Hamiltonian description of a bridge with all possible residual symmetries.

1. Residual σ_v symmetry

An electric field $\mathbf{E} = E \mathbf{e}_z$ normal to the bond's plane reduces the initial C_{2v} symmetry down to $\{E, \sigma_v\}$. This reduction of the symmetry also happens when a molecule is deposited on the surface parallel to the bond plane. While the constraints in Eq. (66) hold, this reduction in symmetry implies the appearance of nonzero in-plane components of $\mathbf{P}_{1,2}$. We parametrize the most general Hubbard model parameters $t_{1,2}$ and $\mathbf{P}_{1,2}$ consistent with the symmetry as

$$t_1 = t_2 = t, \tag{77}$$

$$P_{1,x} = P_{2,x} = p_{xy} \cos \phi, \tag{78}$$

$$P_{1,y} = -P_{2,y} = p_{xy} \sin \phi, \tag{79}$$

$$P_{1,z} = -P_{2,z} = p_z. \tag{80}$$

The effective low energy spin Hamiltonian, derived by Schrieffer-Wolff transformation up to fourth order in t/U, and $|\mathbf{P}|/U$ is given by Eq. (57), with the nonzero parameters,

$$J = \frac{1}{12U^3}[p_{xy}^4 - 2p_{xy}^2 p_z^2 + 3p_z^4 - 8t^2(p_{xy}^2 + 5p_z^2) + 48t^4$$
$$- 8p_{xy}^2(p_z^2 - 4t^2)\cos 2\phi + 2p_{xy}^4 \cos 4\phi], \tag{81}$$

$$D_y = -\frac{p_{xy}}{U^3}(p_z \cos \phi + 2t \sin \phi)(-p_z^2 + 4t^2 + p_{xy}^2 \cos 2\phi), \tag{82}$$

$$D_z = -\frac{1}{2U^3}(4tp_z - p_{xy}^2 \sin 2\phi)(p_z^2 - 4t^2 - p_{xy}^2 \cos 2\phi), \tag{83}$$

$$\Gamma_{xx} = -\frac{1}{6U^3}[p_{xy}^2(1 - \cos 2\phi) + 2p_z^2][8t^2 + p_{xy}^2(1 + \cos 2\phi)], \tag{84}$$

$$\Gamma_{yy} = \frac{1}{12U^3}\{-p_{xy}^4 + 8p_{xy}^2 p_z^2 + 32t^2(p_{xy}^2 - p_z^2)$$
$$+ p_{xy}^2[8(p_z^2 - 4t^2)\cos 2\phi + p_{xy}^2 \cos 4\phi + 48tp_z \sin 2\phi]\}, \tag{85}$$

$$\Gamma_{yz} = \Gamma_{zy} = \frac{p_{xy}}{U^3}(p_z \cos \phi + 2t \sin \phi)(-4tp_z + p_{xy}^2 \sin 2\phi) \tag{86}$$

$$\Gamma_{zz} = -\Gamma_{xx} - \Gamma_{yy}. \tag{87}$$

In the lowest order in spin-orbit coupling the spin interaction consists of the isotropic exchange with $J \approx 4t^4/U^3$, and the Dzyalozhinsky-Moriya interaction with $\mathbf{D} \approx -8t^3(p_{xy} \sin \phi \mathbf{e}_y + p_z \mathbf{e}_z)/U^3$.

As a matter of principle, the spin-orbit coupling mediated hopping $\mathbf{P}$ does not have to be much weaker than the spin-independent hopping t. In this case, all the nonzero terms in Eqs. (81)–(87) are of comparable size, and the variation in spin Hamiltonian with the angle ϕ becomes significant. Note that the angle ϕ describes the directions of spin-orbit coupling induced hopping parameters $\mathbf{P}_{1,2}$, and that it is not directly connected to the bond angle between the magnetic sites and the bridge site. However, for the bridge orbital without azimuthal symmetry, the angle ϕ does depend on the bond angle. For the molecules in which the full symmetry allows only for the spin-electric coupling mediated by the spin-orbit interaction, this effect is important.

With these assumptions, the dependence of the effective spin Hamiltonian on p_{xy} suggests that the strength of induced in-plane Dzyalozhinsky-Moriya vector will be sensitive to the angle ϕ that is determined by the angular dependence of the bridge and magnetic center orbitals. In turn, for a fixed symmetry of the bridge orbital, this dependence directly translates into the dependence of the spin-electric coupling constant on the bridge bond angle.

In the presence of electric field $\mathbf{E} = E \mathbf{e}_z$, the hopping parameters will change from their initial values that satisfy the constraints implied by the C_{2v} symmetry, into a set of values that satisfy those implied by σ_v only. The resulting change in the spin-Hamiltonian parameters reads

$$\delta J = \frac{1}{3U^3}[4t_0(12t_0^2 - 5p_{z0}^2)\delta t + p_{z0}(-20t_0^2 + 3p_{z0}^2)\delta p_z], \tag{88}$$

$$\delta D_y = -\frac{1}{U^3}(4t_0^2 - p_{z0}^2)(2t_0 \sin \phi + p_{z0} \cos \phi)\delta p_{xy}, \tag{89}$$

$$\delta D_z = \frac{2}{U^3}[p_{z0}(12t_0^2 - p_{z0}^2)\delta t + t_0(4t_0^2 - 3p_{z0}^2)\delta p_z], \tag{90}$$

$$\delta\Gamma_{xx} = \delta\Gamma_{yy} = -\frac{1}{2}\delta\Gamma_{zz} = -\frac{16}{3U^3}t_0 p_{z0}(p_{z0}\delta t + t_0\delta p_z),$$
(91)

$$\delta\Gamma_{yz} = \delta\Gamma_{zy} = -\frac{4}{U^3}t_0 p_{z0}(2t_0 \sin\phi + p_{z0}\cos\phi)\delta p_{xy}.$$
(92)

The σ_v-symmetric variations in Hubbard parameters occur when an external electric field is applied along the z direction to a C_{2v} symmetric bond. Again, the variations in the parameters is generically linear in the field strength, $\delta t = \kappa_{t,\sigma v}E_z$, $\delta p_{xy}=\kappa_{pxy,\sigma v}E_z$, and $\delta p_z=\kappa_{pz,\sigma v}E_z$, where the κ parameters depend on the modification of the bridge orbital in the electric field. As opposed to the case of the field along the y direction that maintains the bonds C_{2v} symmetry, the κ parameters for the field along the z axis vanish in zero field since the z component of a vector has no matrix elements between the relevant C_{2v}-symmetric states. The linear expansion is valid when the field is strong enough to distort the bridge orbital. Alternatively, the expansion is valid for a bond with lower symmetry in zero electric field, e.g., when the bond is close to a surface.

2. Residual σ_h symmetry

In an electric field that lies in plane of the bond, with $\mathbf{E}\|\hat{\mathbf{x}}$, the only residual symmetry transformation is the reflection about the xy plane (σ_h). Within this reduced symmetry, the two magnetic sites are no longer equivalent, but the spin-dependent hopping parameters $\mathbf{P}_{1,2}$ still point along the z axis,

$$t_1 \neq t_2, \quad \mathbf{P}_1 = p_1\mathbf{e}_z \neq p_2\mathbf{e}_z = \mathbf{P}_2.$$
(93)

In the fourth order in hopping parameters t and $\mathbf{P}$, the resulting low energy spin Hamiltonian is again given by Eq. (57), with the following nonzero coupling constants:

$$J = \frac{1}{12U^3}[32t_1 t_2 p_{1z}p_{2z} - 4(t_1^2 p_{2z}^2 + t_2^2 p_{1z}^2) + 48t_1^2 t_2^2 + 3p_{1z}^2 p_{2z}^2],$$
(94)

$$\mathbf{D} = -\frac{1}{U^3}(t_1 p_{2z} - t_2 p_{1z})(4t_1 t_2 + p_{1z}p_{2z})\mathbf{e}_z,$$
(95)

$$\Gamma_{xx} = \Gamma_{yy} = -\frac{\Gamma_{zz}}{2} = -\frac{2}{3U^3}(t_1 p_{2z} - t_2 p_{1z})^2.$$
(96)

Similar to the case of full C_{2v} symmetry, the spin Hamiltonian consists of the isotopic exchange J, Dzyalozhinsky-Moriya vector $\mathbf{D}=D_z\hat{\mathbf{z}}$ normal to the bond plane, and diagonal tensor Γ isotropic in the bond plane ($\Gamma_{xx}=\Gamma_{yy}$). We stress that the dependence of the effective spin Hamiltonian parameters on those entering the spin Hubbard Hamiltonian is different for these two symmetries, and so is the response to the applied electric field. On one hand, the C_{2v} preserving electric field induces the transitions in the lowest-energy multiplet in the lowest order. On the other hand, the electric field

that reduces the bond symmetry to $\{E, \sigma_h\}$ does not alter the coupling of spins in the lowest order since the deformation of the molecule requires some coupling to the field.

As in previous case, we expand the σ_h symmetric spin Hamiltonian around the C_{2v} symmetric case. We introduce a perturbation of the parameters Hubbard parameters in the electric field consistent with the residual symmetry: $t_1=t_0 + \delta t_1$, $t_2=t_0+\delta t_2$, $p_{1z}=p_{z0}+\delta p_{1z}$, and $p_{2z}=-p_{z0}+\delta p_{2z}$. As a consequence, the spin Hamiltonian parameters are incremented by

$$\delta J = \frac{1}{6U^3}[4t_0(12t_0^2 - 5p_{z0}^2)(\delta t_1 + \delta t_2) + p_{z0}(-20t_0^2 + 3p_{z0}^2)$$
$$\times(\delta p_{1z} - \delta p_{2z})],$$
(97)

$$\delta D_z = \frac{1}{U^3}[p_{z0}t_0(12t_0 - p_{z0})(\delta t_1 + \delta t_2)$$
$$+ t_0(4t_0^3 - 3p_{z0}^2)(\delta p_{1z} - \delta p_{2z})],$$
(98)

$$\delta\Gamma_{xx} = \delta\Gamma_{yy} = -\frac{\delta\Gamma_{zz}}{2} = -\frac{8}{3U^3}t_0 p_{z0}[p_{z0}(\delta t_1 + \delta t_2)$$
$$+ t_0(\delta p_{1z} - \delta p_{2z})].$$
(99)

As for the case of σ_v residual symmetry, there is no spin-electric effect of the first order in electric field, and the crucial condition for coupling to the electric field in this direction is weak splitting of the bridge orbitals in the molecular field.

3. Residual $R_{y,\pi}$ symmetry

Reduction in the symmetry of the bond, from the full C_{2v} to the group $\{E, R_{y,\pi}\}$, does not occur for any vector perturbation. In terms of electric fields, this reduction in the symmetry would correspond to an inhomogeneous electric field that points in the $\mathbf{e}_z$ direction at the position of one of the magnetic centers, and in the $-\mathbf{e}_z$ direction at the position of the other. This symmetry breaking can also happen when the localized orbitals on the magnetic centers have lobes of opposite signs extending in the z direction and oriented opposite to each other.

The most general Hubbard model parameters consistent with the residual symmetry are

$$t_1 = t_2 = t,$$
(100)

$$P_{1x} = -P_{2x} = p_{xy}\cos\phi,$$
(101)

$$P_{1y} = P_{2y} = p_{xy}\sin\phi,$$
(102)

$$P_{1z} = P_{2z} = p_z.$$
(103)

After the fourth-order Schrieffer-Wolff transformation, the effective low-energy spin Hamiltonian has form (57) with nonzero parameters,

$$J = \frac{1}{12U^3}(p_{xy}^4 - 2p_{xy}^2 p_z^2 + 3p_z^4 - 8t^2(p_{xy}^2 + 5p_z^2) + 48t^2$$
$$+ 8p_{xy}^2(p_z^2 - 4t^2)\cos 2\phi + 2p_{xy}^4\cos 4\phi),$$
(104)

$$D_x = \frac{1}{U^3} p_{xy}(-2t\cos\phi + p_z\sin\phi)(p_z^2 - 4t^2 + p_{xy}^2\cos 2\phi),$$

$$(105)$$

$$D_z = -\frac{1}{2U^3}(4tp_z + p_{xy}^2\sin 2\phi)(p_z^2 - 4t^2 + p_{xy}^2\cos 2\phi),$$

$$(106)$$

$$\Gamma_{xx} = \frac{1}{12U^3}(-p_{xy}^4 + 8p_{xy}^2 p_z^2 + 32t^2(p_{xy}^2 - p_z^2)$$
$$+ p_{xy}^2[-8(p_z^2 - 4t^2)\cos 2\phi + p_{xy}^2\cos 4\phi$$
$$- 48tp_z\sin 2\phi]),$$

$$(107)$$

$$\Gamma_{zx} = \Gamma_{xz} = \frac{1}{U^3}p_{xy}(2t\cos\phi - p_z\sin\phi)(4tp_z + p_{xy}^2\sin 2\phi),$$

$$(108)$$

$$\Gamma_{yy} = \frac{1}{6U^3}[p_{xy}^2(1 + \cos 2\phi) + 2p_z^2][p_{xy}^2(-1 + \cos 2\phi) - 8t^2],$$

$$(109)$$

$$\Gamma_{zz} = -\Gamma_{xx} - \Gamma_{yy} = -\frac{1}{6U^3}\{-p_{xy}^4 + 2p_{xy}^2 p_z^2 + 8t^2(p_z^2 - 4p_z^2)$$
$$+ p_{xy}^2[-2(p_z^2 - 4t^2)\cos 2\phi + p_{xy}^2\cos 4\phi - 24tp_z\sin 2\phi]\}.$$

$$(110)$$

The expansion from the C_{2v} symmetric case gives (see the discussion of the σ_v residual symmetry in Sec. III D 1,

$$\delta J = \frac{1}{3U^3}[4t_0(12t_0^2 - 5p_{z0}^2)\delta t + p_{z0}(-20t_0^2 + 3p_{z0}^2)\delta p_z],$$

$$(111)$$

$$\delta D_x = \frac{1}{U^3}(4t_0^2 - p_{z0}^2)(2t_0\cos\phi_0 - p_{z0}\sin\phi_0)\delta p_{xy},$$

$$(112)$$

$$\delta D_z = \frac{2}{U^3}[p_{z0}(12t_0^2 - p_{z0}^2)\delta t + t_0(4t_0^2 - 3p_{z0}^2)\delta p_{z0}],$$

$$(113)$$

$$\delta\Gamma_{xx} = \delta\Gamma_{yy} = -\frac{1}{2}\delta\Gamma_{zz} = -\frac{16}{3U^3}p_{z0}t_0(p_{z0}\delta t + t_0\delta p_z),$$

$$(114)$$

$$\delta\Gamma_{zx} = \delta\Gamma_{xz} = \frac{4}{U^3}t_0 p_{z0}(2t_0\cos\phi_0 - p_{z0}\sin\phi_0)\delta p_{xy}.$$

$$(115)$$

As in the case of σ_v symmetry, the resulting interaction of the spins on magnetic centers becomes dependent on the

angle ϕ between the two **P** parameters. This dependence is pronounced in the case of strong spin-orbit coupling and can lead to the dependence of spin-electric effects on both the geometry of the bond and the shape of the bridge orbital.

E. Bond modification and symmetries

Spin-electric coupling induced by the superexchange through bridge atoms depends on the symmetry of the bridge and the direction of the electric field. This symmetry reflects on the resulting coupling of spins in an MN. In this section, we combine the results of the Hubbard model study of the individual bonds with the previous symmetry considerations and provide rough estimates of the most promising spin-electric coupling mechanism in the triangular and pentagonal molecules.

The spin-electric coupling via superexchange is most sensitive to the electric fields that does not break the initial C_{2v} local symmetry of the bond. This symmetry corresponds to the electric field that lies in the plane of the molecule and normal to the bond. All the other couplings require modification of the bridge orbitals and are suppressed by a factor $d|\mathbf{E}|/U_d$, where U_d is on-site repulsion on the bridge. Assuming that this repulsion is strong, we can model the spin electric coupling as a set of modifications of the spin interactions δH_{jj+1} between the neighboring magnetic centers, with $\|\delta H_{jj+1}\| \propto |E_\perp^{\text{bond}}|$, where $E_\perp^{\text{bond}}$ is the projection of the electric field normal to the bond and lying in the molecule's plane.

In the triangle, the strongest effects of electric field is modification of exchange couplings $\delta J_{jj+1} = \delta J_0\cos(2j\pi/3 + \theta_0)$, where the angle θ_0 describes the orientation of the in-plane component of the electric field, and δJ_0 is a molecule-dependent constant. This modification leads to a specific coupling of the in-plane components of chirality to the electric field $H_{e-d}^{\text{eff}} = d\mathbf{E}' \cdot \mathbf{C}_\|$, see Eq. (7). Other types of coupling are suppressed either due to weaker influence of electric field on the bonds or due to the symmetry of the molecule. If the spin-electric coupling is mediated by the spin-orbit interaction, the suppression is by a factor of the order $|\mathbf{D}|/J$, and if the coupling is mediated by electric field, the suppression factor is $d|\mathbf{E}|/J$. Assuming the simplest case, the modification of exchange coupling is the most promising mechanism for spin-electric coupling in triangular molecules.

In the pentagons, the modification of spin-spin interaction δH_{jj+1} preferred by the superexchange mechanism is inefficient in inducing the spin-electric coupling of the molecule. The pattern δJ_{jj+1} of exchange coupling constants induced by an external electric field does not couple the states within the lowest energy manifold. In order to couple the spins in the pentagon to an external field, another mechanism is needed. The modification of the Dzyalozhinsky-Moriya vectors $\delta D_{jz} = \delta D_{z0}\cos(2j\pi/5 + \theta_0)$, where δD_{z0} is a molecule-dependent constant, and θ_0 describes the orientation of the in-plane component of the electric field, are preferred by the superexchange bridge model. In the symmetry analysis, we have found that this form of modification of spin-orbit coupling does not induce spin-electric coupling. The same applies to the modifications of in-plane components $D_{jj+1,x(y)}$.

The main effect that gives rise to spin-electric coupling is the modification of the exchange interactions δJ_{jj+1} in the presence of the original spin-orbit interaction $D_{jj+1,z}$. Compared to a triangle composed out of identical bonds, this interaction will be weaker by a factor of $|\mathbf{D}_{jj+1}|/J_{jj+1}$.

In summary, within our model of the superexchange-mediated spin-electric coupling, the most promising candidates for the spin manipulation via electric field are triangular molecules. In pentagons, the best candidates are molecules with strong spin-orbit interaction, and weakly split bridge orbitals.

IV. EXPERIMENTAL SIGNATURES OF THE SPIN-ELECTRIC COUPLING

Coherent quantum control of spins in an MN using electric fields can be achieved by resonant driving of the transitions between the chirality eigenstates.[42] At present, however, little is known about the effects of electric fields on the spin states of molecular magnets. As a preliminary step, it is thus useful to identify possible signatures of such a coupling that are observable in the experiments routinely used to characterize these systems.

In this section, we study the ways in which the spin-electric coupling can be detected in electron spin resonance (ESR), in nuclear magnetic resonance (NMR), and in the thermodynamic measurement of an MN.

A. Electron spin resonance

ESR investigates transitions between states belonging to a given S multiplet and having different spin projections M along the magnetic field direction.[67] This technique provides information on the anisotropies of the spin system, as well as on the chemical environment, and the spin dynamics.[29] In the following, we show how the effects of an external electric field can show up in the ESR spectra of antiferromagnetic spin rings by affecting both the frequency and the oscillator strength of the transitions.

1. Triangle of s = 1/2 spins

We start by considering the simplest case of interest, namely, that of a triangle of $s=1/2$ spins with D_{3h} symmetry. The lowest energy eigenstates of the spin triangle, given in Eq. (3) form an $S=1/2$ quadruplet. The effective Hamiltonian H_{eff} of the molecule in the presence of electric and magnetic fields within this quadruplet is given by Eq. (15).

We first consider the case of a static magnetic field perpendicular to the molecule's plane ($\mathbf{B}\|\hat{\mathbf{z}}$). The eigenvalues of H_{eff} are then given by

$$\lambda_\sigma^\alpha = \sigma[\mathcal{B} + \alpha(\Delta_{\text{SO}}^2 + \mathcal{E}^2)^{1/2}], \tag{116}$$

where $\mathcal{E}\equiv d|\mathbf{E}\times\hat{\mathbf{z}}|$, $\mathcal{B}=\mu_B\sqrt{g_\|^2 B_z^2+g_\perp^2 B_\perp^2}$, $\sigma=\pm 1/2$ is the eigenvalue of S_z, and $\alpha=\pm 1$ is the eigenstate chirality in the limit of vanishing electric field. In fact, $|\lambda_\sigma^\alpha\rangle_{\mathcal{E}=0}$ coincides with $|\alpha,\sigma\rangle$ up to a phase factor. In the presence of electric field, the eigenstates read
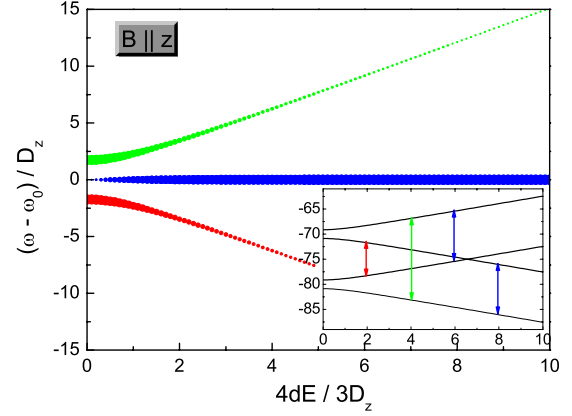

FIG. 7. (Color online) Energy (ω) of the ESR transitions in a triangle of $s=1/2$ spins as a function of the applied electric field $\mathbf{E}$ that lies in the molecule's plane so that $d|\mathbf{E}|=dE=\mathcal{E}$. The magnetic field is $\mathbf{B}\|\hat{\mathbf{z}}$ and $\omega_0=g\mu_B B$, see Eqs. (120) and (121). The diameter of the circles is proportional to the transition amplitudes $|\langle\alpha|S_x|\alpha'\rangle|$, Eqs. (118) and (119). Here, $|\alpha\rangle$ are the eigenstates of H in the lowest energy $S=1/2$ multiplet. Inset: eigenvalues (in units of D_z) as a function of $\mathcal{E}=d|\mathbf{E}_\||$, in units $3D_z/4$.

$$|\lambda_\sigma^\alpha\rangle = \{2\sigma[\Delta_{\text{SO}} + \alpha(\mathcal{E}^2 + \Delta_{\text{SO}}^2)^{1/2}]|+1,\sigma\rangle + \mathcal{E}e^{-i\theta}|-1,\sigma\rangle\}/D^\alpha, \tag{117}$$

where $D^\alpha=\{\mathcal{E}^2+[\Delta_{\text{SO}}+\alpha(\mathcal{E}^2+\Delta_{\text{SO}}^2)^{1/2}]^2\}^{1/2}$.

Electron spin resonance induces transitions between such eigenstates. The transition amplitudes are given by the absolute values of matrix elements of x component of the total spin, taken between the states that the transition connects,

$$\langle\lambda_{-1/2}^\alpha|S_x|\lambda_{+1/2}^{-\alpha}\rangle = -\mathcal{E}^2/D^{+1}D^{-1}, \tag{118}$$

$$\langle\lambda_{-1/2}^\alpha|S_x|\lambda_{+1/2}^\alpha\rangle = \frac{\Delta_{\text{SO}}[\Delta_{\text{SO}} + \alpha(\mathcal{E}^2 + \Delta_{\text{SO}}^2)^{1/2}]}{(D^\alpha)^2}. \tag{119}$$

The corresponding frequencies are given by

$$\lambda_{+1/2}^\alpha - \lambda_{-1/2}^{-\alpha} = \mathcal{B}, \tag{120}$$

$$\lambda_{+1/2}^\alpha - \lambda_{-1/2}^\alpha = \mathcal{B} + \alpha(\mathcal{E}^2 + \Delta_{\text{SO}}^2)^{1/2}. \tag{121}$$

As an illustrative example, we plot the frequencies and amplitudes of the ESR transitions as a function of the electric field (Fig. 7). While for $\mathcal{E}=0$, these transitions can only take place between states of equal C_z (red and green symbols online, transitions with the larger amplitude at low fields, in the figure and in the inset), the electric field mixes states of opposite chirality, thus transferring oscillator strength to two further transitions, whose frequencies are independent of $\mathcal{E}$ (blue symbols online, constant frequency transition in the figure). In the limit $dE\gg D_z$, the eigenstates of the spin Hamiltonian tend to coincide with those of $\mathbf{S}_{12}^2$, and ESR transitions take place between states of equal S_{12}. While the eigenstates depend on the in-plane orientation of the electric field, no such dependence is present in the frequencies and oscillator strength of the ESR transitions. Besides, these quantities are independent of the exchange coupling J and

depend on the value of the applied magnetic field only through an additive constant (ω_0).

The dependence of the ESR spectrum on the applied electric field is qualitatively different if the static magnetic field is applied in-plane (e.g., $\mathbf{B} \| \hat{\mathbf{x}}$ and the oscillating field oriented along $\hat{\mathbf{z}}$). In this case, the eigenvalues of H_{eff} are

$$\mu_\sigma^\alpha = \alpha\sigma[\Delta_{\text{SO}}^2 + (\mathcal{E} + \alpha\mathcal{B})^2]^{1/2}, \quad (122)$$

where $\sigma = \pm 1/2$ is the value of $\langle S_x \rangle$ in the limit of large magnetic field ($\mathcal{B} \gg \mathcal{E}, \Delta_{\text{SO}}$) and $\alpha = \pm 1$. The corresponding eigenstates read

$$|\mu_\sigma^\alpha\rangle = \{e^{i\theta}(\Delta_{\text{SO}} + \mu_\sigma^\alpha)[|+1, +1/2\rangle - |-1, -1/2\rangle]$$
$$+ (\mathcal{B} + \alpha\mathcal{E})[|+1, -1/2\rangle - |-1, +1/2\rangle]\}/D_\sigma^\alpha,$$
$$(123)$$

where

$$D_\sigma^\alpha = \sqrt{2}[(\Delta_{\text{SO}} + \mu_\sigma^\alpha)^2 + (\mathcal{B} + \alpha\mathcal{E})^2]^{1/2}. \quad (124)$$

The expectation values of the total spin along the magnetic field for each of the above eigenstates are given by the following expressions

$$\langle\mu_\sigma^\alpha|S_x|\mu_\sigma^\alpha\rangle = 2[(\Delta_{\text{SO}} + \mu_\sigma^\alpha)(\mathcal{B} - \alpha\mathcal{E})]/(D_\sigma^\alpha)^2, \quad (125)$$

which are independent of the in-plane direction of the electric field. The ESR transitions between such eigenstates induced by a magnetic field that oscillates along the z direction are given by the expressions

$$\langle\mu_\sigma^\alpha|S_z|\mu_{\sigma'}^{-\alpha}\rangle = \frac{(\Delta_{\text{SO}} + \mu_\sigma^\alpha)(\Delta_{\text{SO}} + \mu_{\sigma'}^{-\alpha}) + (\mathcal{E}^2 - \mathcal{B}^2)}{D^\alpha D^{-\alpha}},$$

$$\langle\mu_\sigma^\alpha|S_z|\mu_{\sigma'}^{\alpha}\rangle = 0. \quad (126)$$

Therefore, the application of the electric field shifts the energy of the transitions between states of opposite α, thus removing their degeneracy; however, unlike the case $\mathbf{B} \| \hat{\mathbf{z}}$, it does not increase the number of allowed transitions.

In the case of tilted magnetic fields, the dependence of the ESR spectrum on the applied electric field presents qualitatively different features (Fig. 8). In particular, the spectrum is dominated by two pairs of degenerate transitions that anti-cross as a function of the electric field. Away from the anti-crossing, the transitions with the largest oscillator strength display frequency dependence on the electric field.

2. Pentagons of s = 1/2 spins

Triangles of $s = 3/2$ spins (not shown here) display the same qualitative behavior as the one discussed above. In contrast, chains including an odd number $N > 3$ spins behave differently. This is mainly due to the fact that the spin-electric coupling δH does not couple directly the four eigenstates of H belonging to the lowest $S = 1/2$ multiplet: such coupling only takes place through mixing with the higher $S = 1/2$ multiplet. As a consequence, the effects of the spin-electric coupling tend to be weaker as compared to the case of the triangle; besides, unlike the above case of the spin
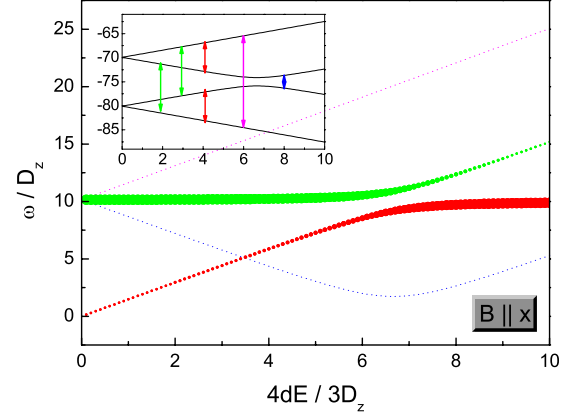

FIG. 8. (Color online) Energy (ω) of the ESR transitions in a triangle of $s = 1/2$ spins as a function of the applied in-plane electric field $\mathbf{E}$ so that $d|\mathbf{E}| = dE = \mathcal{E}$, and in the presence of the in-plane magnetic field $\mathbf{B} \| \hat{\mathbf{x}}$. The diameter of the circles is proportional to $|\langle\alpha|S_z|\alpha'\rangle|$, Eqs. (120) and (121). The states $|\alpha\rangle$ are the eigenstates of H in the lowest $S = 1/2$ multiplet. Inset: eigenvalues (in units of D_z) as a function of $d|\mathbf{E}_\|| = \mathcal{E}$, in units $3D_z/4$.

triangle, they depend on the exchange coupling J. Illustrative numerical results are shown in Figs. 9 and 10 for the cases of a perpendicular and in-plane magnetic field, respectively. In the former case, both the frequencies and amplitude of the ESR transitions are hardly affected by the electric field in the same range of physical parameters considered in Fig. 7. In the case of an in-plane magnetic field, instead, a relatively small shift in the transition energies is accompanied by a strong transfer of the oscillator strength for values of the spin-electric coupling exceeding the Dzyalozhinsky-Moriya coupling constant.
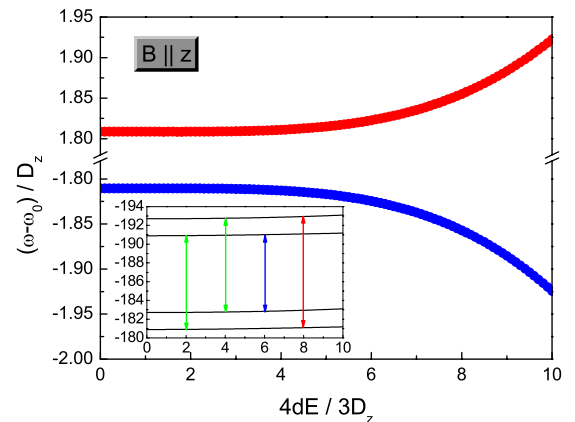

FIG. 9. (Color online) Energy (ω) of the ESR transitions in a pentagon of $s = 1/2$ spins as a function of the electric field applied in the molecule's plane $d|\mathbf{E}| = dE = \mathcal{E}$. The Zeeman splitting, $\omega_0 = g\mu_B B$ is set by the magnetic field $\mathbf{B} \| \hat{\mathbf{z}}$, orthogonal to the molecule's plane. The considered transitions are those between eigenstates ($|\alpha\rangle$) belonging to the $S = 1/2$ multiplet of the spin Hamiltonian (figure inset). Unlike the case of the spin triangle, these are coupled to each other by the electric field via eigenstates belonging to other multiplets, and therefore depends also on the exchange constant J (here $J/\Delta_{\text{SO}} = 100$). The diameter of the circles is proportional to $|\langle\alpha|S_x|\alpha'\rangle|$, and therefore to the transition amplitude.
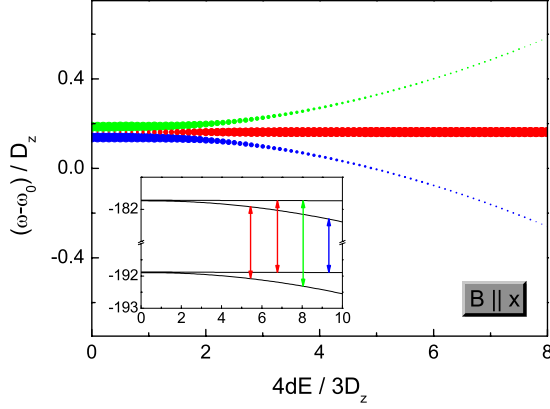
FIG. 10. (Color online) Energy (ω) of the ESR transitions in a pentagon of $s=1/2$ spins as a function of the applied in-plane electric field **E** so that $d|\mathbf{E}|=dE=\mathcal{E}$. The Zeeman splitting is set by an in-plane magnetic field $\mathbf{B}\|\hat{\mathbf{x}}$, and $\omega_0=g\mu_B B$. The considered transitions are those between eigenstates ($|\alpha\rangle$) belonging to the $S=1/2$ multiplet of the spin Hamiltonian (figure inset). Unlike the case of the spin triangle, these are coupled to each other by the electric field via eigenstates belonging to other multiplets and therefore depends also on the exchange constant J (here $J/\Delta_{SO}=100$). The diameter of the circles is proportional to $|\langle\alpha|S_z|\alpha'\rangle|$, and therefore to the transition amplitude.

B. Nuclear magnetic resonance

The spin-electric Hamiltonian δH_0 modifies nonuniformly the superexchange couplings between neighboring spins. This might not affect the projection of the total spin (as in the case $\mathbf{B}\|\hat{\mathbf{z}}$, see above), but it generally affects the moment distribution within the spin chain. Such effect can be investigated through experimental techniques that act as local probes in molecular nanomagnets, such as NMR (Ref. 68) or x-ray absorption.[69] In NMR, the expectation value of a given spin within the cluster can be inferred through the frequency shift induced on the transitions of the corresponding nucleus. The shift in the nuclear resonance frequency for the nucleus of the i-th magnetic ion is $\Delta\nu=\gamma A\langle s_{z,i}\rangle$, where A is the contact hyperfine interaction constant at the nuclear site. The constant of proportionality A depends on the spin density at the position of the nucleus and can be extracted from the experiment by considering the polarized ground state $M=S$ at high magnetic fields.[68] As in the case of ESR, the dependence of the NMR spectra on the applied electric field qualitatively depends on the orientation of the static magnetic field **B** with respect to the molecule. Unlike the case of ESR, however, it also depends on the in-plane orientation of the electric field, i.e., on the way in which the **E** breaks the symmetry of the molecule.

1. Spin triangles

Let us start by considering a spin $s=1/2$ triangle, with a magnetic field applied perpendicular to the molecule plane ($\mathbf{B}\|\hat{\mathbf{z}}$). In this case, the distribution of the spin projection along z is given by the following expression:
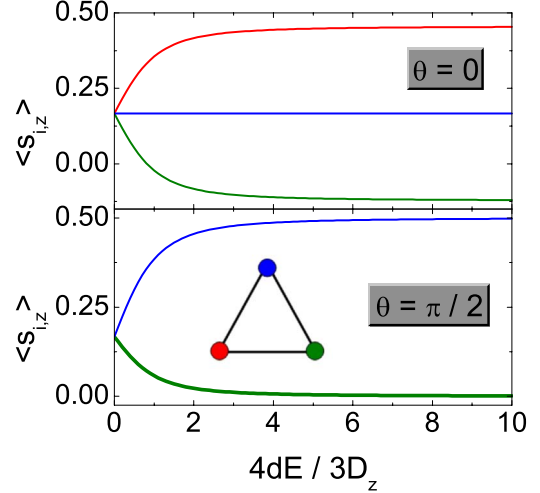

FIG. 11. (Color online) Expectation values of the z component of $s=1/2$ spins in a triangular molecule as a function of applied electric field. The magnetic field is perpendicular to the ring plane ($\mathbf{B}\|\hat{\mathbf{z}}$); the electric field is parallel and perpendicular to $\mathbf{r}_{12}$ in the upper and lower panel, respectively. In the electric field along one of the bonds (lower panel), the spins that lie on that bond have the same out-of-plane projections. The shadings (colors online) denote the different spins.

$$\langle\lambda_\sigma^\alpha|s_{i,z}|\lambda_\sigma^\alpha\rangle = \sigma/3 + f_\sigma^\alpha(\mathcal{E})\cos[\theta + \pi(5/3-i)], \quad (127)$$

where

$$f_\sigma^\alpha(\mathcal{E}) \equiv \frac{4\sigma\mathcal{E}[\Delta_{SO} + \alpha(\Delta_{SO}^2 + \mathcal{E}^2)^{1/2}]}{3(D^\alpha)^2}. \quad (128)$$

Here, the expressions of the eigenstates $|\lambda_\sigma^\alpha\rangle$ and of D^α are given in Sec. IV A. For $E=0$, the three spins are equivalent and $\langle\lambda_{\pm1/2}^\alpha|s_{i,z}|\lambda_{\pm1/2}^\alpha\rangle = \pm 1/6$. If the electric field is finite and oriented along one of the triangle sides (e.g., $\mathbf{E}\|\mathbf{r}_{12}$, corresponding to $\theta=0$), then expectation values along z of spins 1 and 2 undergo opposite shifts, whereas that of spin 3 is left unchanged: $\Delta_\mathbf{E}\langle s_{1,z}\rangle=-\Delta_\mathbf{E}\langle s_{2,z}\rangle$, where $\Delta_\mathbf{E}\langle s_{i,z}\rangle\equiv\langle s_{i,z}\rangle_\mathbf{E} - \langle s_{i,z}\rangle_{\mathbf{E}=0}$. This is shown in Fig. 11 for the ground state of the spin Hamiltonian, but the above relations hold for any of the four eigenstates $|\lambda_\sigma^\alpha\rangle$ belonging to the $S=1/2$ quadruplet. If the NMR frequency shifts $\Delta\nu_i$ are larger than the corresponding line widths, the single line at $\mathbf{E}=0$ splits into three equispaced lines, with intensity ratios 1:1:1. If, instead, the electric field is applied along a symmetry plane of the triangle (e.g., $\mathbf{E}\perp\mathbf{r}_{12}$, corresponding to $\theta=\pi/2$), spins 1 and 2 remain equivalent and their magnetic moments display the same electric field dependence, while the shift of the third one is opposite in sign and twice as large in absolute value: $\Delta_\mathbf{E}\langle s_{1,z}\rangle=\Delta_\mathbf{E}\langle s_{2,z}\rangle=-\Delta_\mathbf{E}\langle s_{3,z}\rangle/3$. The intensity ratios of the two NMR lines are, correspondingly, 1:2. The expectation values for the remaining eigenstates can be derived by the following equations: $\Delta_\mathbf{E}\langle\lambda_{-1/2}^\alpha|s_{i,z}|\lambda_{-1/2}^\alpha\rangle=-\Delta_\mathbf{E}\langle\lambda_{+1/2}^\alpha|s_{i,z}|\lambda_{+1/2}^\alpha\rangle$ and $\langle\lambda_\sigma^1|s_{i,z}|\lambda_\sigma^1\rangle=-\Delta_\mathbf{E}\langle\lambda_\sigma^{-1}|s_{i,z}|\lambda_\sigma^{-1}\rangle$. Therefore, at finite temperature, the shifts in the expectation values of the three spins are given by
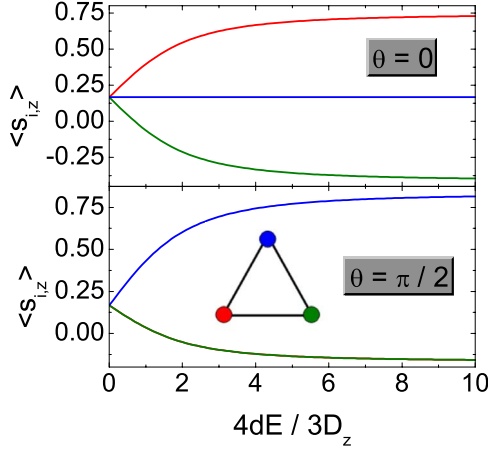
FIG. 12. (Color online) Expectation values of the z component of $s=3/2$ spins in a triangular molecule as a function of applied electric field. The magnetic field is perpendicular to the ring plane ($\mathbf{B}\|\hat{\mathbf{z}}$); the electric field is parallel and perpendicular to $\mathbf{r}_{12}$ in the upper and lower panels, respectively. The shadings denote the different spins.

$$\frac{\Delta_{\mathbf{E}}\langle s_{i,z}\rangle}{\Delta_{\mathbf{E}}\langle\lambda^{+1}_{-1/2}|s_{i,z}|\lambda^{+1}_{-1/2}\rangle} = \frac{\displaystyle\sum_{\alpha}\alpha\cosh\left(\frac{\lambda^{\alpha}_{-1/2}}{k_B T}\right)}{\displaystyle\sum_{\alpha}\cosh\left(\frac{\lambda^{\alpha}_{-1/2}}{k_B T}\right)}. \qquad (129)$$

If the field is oriented along the molecule plane ($\mathbf{B}\|\hat{\mathbf{x}}$), the expectation value of the three spins corresponding to each of the eigenstates are given by the following expressions:

$$\langle\mu^{\alpha}_{\sigma}|s_{i,x}|\mu^{\alpha}_{\sigma}\rangle = g^{\alpha}_{\sigma}(\mathcal{E}) + (1/3)\cos(\theta - 2i\pi/3), \qquad (130)$$

where

$$g^{\alpha}_{\sigma}(\mathcal{E}) \equiv \frac{2}{3}\frac{(\Delta_{\mathrm{SO}} + \mu^{\alpha}_{\sigma})(\mathcal{B} + \alpha\mathcal{E})}{(D^{\alpha})^2}. \qquad (131)$$

If the magnetic field is parallel to the triangle plane, the in-plane electric field can modify the total spin expectation value along $\mathbf{B}$. The changes that $\mathbf{E}$ induces in the magnetization distribution within the triangle at zero temperature are less varied than in the previous case (Fig. 11). In fact, the magnitude of the $\Delta_{\mathbf{E}}\langle s_{i,z}\rangle$ is much smaller, and all the spins undergo shifts of equal sign and slope. The NMR line, which is slitted into three lines already for $\mathbf{E}=0$, is rigidly shifted by the applied electric field.

If the triangle is formed by half-integer spins $s > 1/2$, an analogous dependence of the expectation values $\langle s_{i,z}\rangle$ on the electric field is found. As an illustrative example, we report in Fig. 12 the case of $s=3/2$.

2. Pentagon of $s=1/2$ spins

Spin chains consisting of an odd number of half-integer spins present analogous behaviors but also meaningful differences with respect to the case of the spin triangle. In particular, the spin-electric Hamiltonian δH_0 does not couple states belonging to the lowest $S=1/2$ quadruplet directly
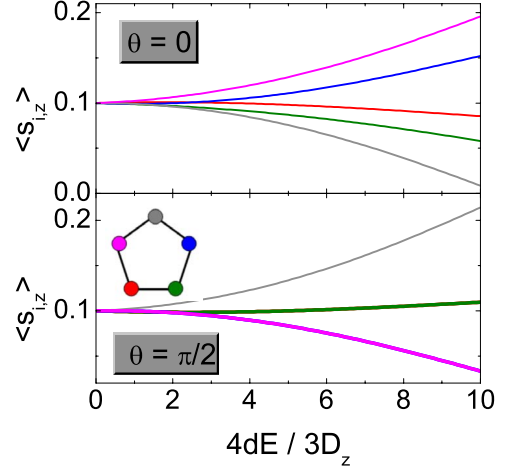

FIG. 13. (Color online) Expectation values of the z component of $s=1/2$ spins in a pentagon as a function of applied electric field. The magnetic field is perpendicular to the ring plane ($\mathbf{B}\|\hat{\mathbf{z}}$); the electric field is parallel ($\theta=0$) and perpendicular ($\theta=\pi/2$) to $\mathbf{r}_{12}$ in the upper and lower panel, respectively. The shadings (colors online) denote the different spins.

(i.e., matrix elements $\langle i|\delta H_0|j\rangle=0$ for $i,j\leq 4$); these couplings are mediated by states belonging to higher $S=1/2$ multiplets that are higher in energy by a quantity $\sim J$. Therefore, the effect of the electric field tends to be significantly smaller than in the case of a triangle with equal D_z and $\mathcal{E}$ (see Fig. 13) and depends also on the exchange coupling J.

C. Magnetization, polarization, and susceptibilities

The spin-electric coupling shifts the energy eigenvalues of the nanomagnet, thus affecting thermodynamic quantities, such as magnetization, polarization, and susceptibilities. In the following, we compute these quantities in the case of the $s=1/2$ spin triangle as a function of the applied magnetic and electric fields. Under the realistic assumption that the exchange splitting J is the largest energy scale in the spin Hamiltonian, and being mainly interested in the low-temperature limit, we restrict ourselves to the $S=1/2$ quadruplet, and use the effective Hamiltonian H_{eff} in Eq. (21).

The eigenenergies of the lowest $S=1/2$ sector in the presence of electric and magnetic fields are

$$E_{\alpha,\gamma} = \alpha\gamma\sqrt{\mathcal{B}^2 + \Delta^2_{\mathrm{SO}} + \mathcal{E}^2 + 2\gamma E^2_0}, \qquad (132)$$

with $\mathcal{B}=\mu_B\sqrt{g^2_{\|}H^2_{\|}+g^2_{\perp}H^2_{\perp}}$, $E_0=[(\mathcal{B}_z\Delta_{\mathrm{SO}})^2+(\mathcal{B}\mathcal{E})^2]^{1/4}$, and $\mathcal{B}_z=\mu_B g_{\|}H_{\|}$. Note that these energies are the generalization of the ones in the previous section, which were valid for in-plane magnetic field only, and that the magnetic field $B_i \equiv \mu_0 H_i$, with $i=x,y,z$. The partition function for N identical and noninteracting molecules is $Z=Z^N_1$, with $Z_1 =\Sigma_{\alpha,\gamma}\exp(-\beta E_{\alpha,\gamma})$ being the partition function for one molecule, and $\beta=1/(k_B T)$. The free energy reads

$$F \equiv -1/\beta\ln Z = -Nk_B T\ln\left[2\sum_{\gamma}\cosh(\beta E_{\gamma})\right], \qquad (133)$$

with $E_{\gamma}\equiv E_{1/2,\gamma}$. From this, we can derive different thermodynamic quantities like the magnetization $M_i=-\partial F/\partial H_i$, the

electric polarization $P_i = -\partial F/\partial E_i$, the heat capacity $C = -\partial/\partial T(\partial \ln(Z)/\partial \beta)$, and the corresponding susceptibilities: $\chi_{E_i E_j} = \partial P_i/\partial E_j = \partial^2 F/\partial E_i \partial E_j$—the *electric* susceptibility, $\chi_{B_i B_j} = \partial M_i/\partial H_j = \partial^2 F/\partial H_i \partial H_j$—the *spin* susceptibility, and $\chi_{E_i B_j} = \partial P_i/\partial M_j = \partial^2 F/\partial E_i \partial H_j$—the *spin-electric* susceptibility. For the electric polarization components P_i we get

$$P_i = \frac{Nd\mathcal{E}_i}{4 \sum\limits_{\gamma = \pm 1} \cosh(\beta E_\gamma)} \sum_{\gamma = \pm 1} \frac{\sinh(\beta E_\gamma)}{E_\gamma}$$
$$\times \left(1 + \gamma \frac{\mathcal{B}^2}{E_0^2} \right)(1 - \delta_{i,z}), \tag{134}$$

while for the magnetization components M_i we get

$$M_i = \frac{Ng_i\mu_B\mathcal{B}_i}{2 \sum\limits_{\gamma = \pm 1} \cosh(\beta E_\gamma)} \sum_{\gamma = \pm 1} \frac{\sinh(\beta E_\gamma)}{E_\gamma}$$
$$\times \left(1 + \gamma \frac{\Delta_{\mathrm{SO}}^2 \delta_{i,z} + \mathcal{E}^2}{E_0^2} \right), \tag{135}$$

where again $i = x, y$. Making use of the above expressions, we can obtain the above defined susceptibilities

$$\chi_{E_i E_j} = \frac{P_i}{E_j}\delta_{ij} - \beta P_i P_j + \frac{Nd^4 E_i E_j}{2 \sum\limits_{\gamma = \pm 1} \cosh(\beta E_\gamma)}$$
$$\times \left[\sum_{\gamma = \pm 1} \frac{\beta E_\gamma \cosh(\beta E_\gamma) - \sinh(\beta E_\gamma)}{2E_\gamma^3} \left(1 + \gamma \frac{\mathcal{B}^2}{E_0^2} \right)^2 \right.$$
$$\left. + \gamma \frac{\mathcal{B}^4}{E_0^6} \frac{\sinh(\beta E_\gamma)}{E_\gamma} \right] = \chi_{E_j E_i}, \tag{136}$$

$$\chi_{B_i B_j} = \frac{M_i}{B_j}\delta_{ij} - \beta M_i M_j + \frac{Ng_i^2 g_j^2 B_i B_j}{2 \sum\limits_{\gamma = \pm 1} \cosh(\beta E_\gamma)} \sum_{\gamma = \pm 1} \left[\frac{(\Delta_{\mathrm{SO}}^2\delta_{i,z} + \mathcal{E}^2)(\Delta_{\mathrm{SO}}^2\delta_{j,z} + \mathcal{E}^2)}{E_0^6} \frac{\sinh(\beta E_\gamma)}{E_\gamma} + \frac{\beta E_\gamma \cosh(\beta E_\gamma) - \sinh(\beta E_\gamma)}{2E_\gamma^3} \right.$$
$$\left. \times \left(1 + \gamma \frac{\Delta_{\mathrm{SO}}^2\delta_{i,z} + \mathcal{E}^2}{E_0^2} \right) \left(1 + \gamma \frac{\Delta_{\mathrm{SO}}^2\delta_{j,z} + \mathcal{E}^2}{E_0^2} \right) \right] = \chi_{B_j B_i}, \tag{137}$$

$$\chi_{B_i E_j} = -\beta M_i P_j + \frac{Ng_i^2 d^2 B_i E_j}{2 \sum\limits_{\gamma = \pm 1} \cosh(\beta E_\gamma)} \sum_{\gamma = \pm 1} \left[\gamma \frac{(\Delta_{\mathrm{SO}}^2\delta_{i,z} + \mathcal{E}^2)(\Delta_{\mathrm{SO}}^2\delta_{j,z} + \mathcal{E}^2)}{E_0^6} \frac{\sinh(\beta E_\gamma)}{E_\gamma} + \frac{\beta E_\gamma \cosh(\beta E_\gamma) - \sinh(\beta E_\gamma)}{2E_\gamma^3} \right.$$
$$\left. \times \left(1 + \gamma \frac{\Delta_{\mathrm{SO}}^2\delta_{i,z} + \mathcal{E}^2}{E_0^2} \right) \left(1 + \gamma \frac{\mathcal{B}^2}{E_0^2} \right) \right] (1 - \delta_{j,z}) = \chi_{E_j B_i}. \tag{138}$$

The polarization **P**, magnetization **M**, and susceptibilities χ, Eqs. (134)–(138), all depend on the spin-electric coupling constant d. In the following, we analyze the details of this dependence and identify the conditions suitable for extracting the value of d from the measurable quantities.

1. Polarization and magnetization

The in-plane polarization of the molecule as a function of the magnetic field is illustrated in Figs. 14 and 15. The polarization is a growing function of the magnetic field strength, and it gets reduced by the normal component of the field.

The low-temperature, $k_B T \ll \Delta_{\mathrm{SO}}$, thermodynamic properties of a molecule with spin-electric coupling show a simple dependence on the strength of external electric and magnetic fields in the special cases of in-plane and out-of plane magnetic fields. We focus only on effects in leading orders in electric field under the realistic assumption that the electric dipole splitting is small compared to the SO splitting, i.e.,

$\mathcal{E} \ll \Delta_{\mathrm{SO}}$. Also, we analyze two limiting cases: (i) $k_B T \ll \mathcal{E}$, i.e., low-temperature regime, and (ii) $k_B T \gg \mathcal{E}$, i.e., high temperature regime. However, we assume all temperatures (in both regimes) to satisfy $k_B T \ll \Delta_{\mathrm{SO}}$ so that the spin-orbit split levels are well resolved. In the first case (i), we obtain for the polarization

$$P_i \simeq \begin{cases} \dfrac{nd\mathcal{E}_i\mathcal{B}}{4\mathcal{E}\Delta_{\mathcal{B}}} & \text{for } \mathcal{E} \ll \mathcal{B} \\[2mm] \dfrac{nd\Delta_{\mathrm{SO}}^2\mathcal{E}_i}{4\Delta_{\mathcal{B}}^3} & \text{for } \mathcal{E} \gg \mathcal{B}, \end{cases} \tag{139}$$

while for the second situation (ii) we obtain

$$P_i \simeq \frac{nd\Delta_{\mathrm{SO}}^2\mathcal{E}_i}{4\Delta_{\mathcal{B}}^3} \left(1 + \frac{\mathcal{B}^2}{\Delta_{\mathrm{SO}}^2}\beta\Delta_{\mathcal{B}} \right), \tag{140}$$

with $\Delta_{\mathcal{B}} = \sqrt{\mathcal{B}^2 + \Delta_{\mathrm{SO}}^2}$ and $n = N/V$ the density of molecules in the crystal. We see that, for low temperatures, the electric
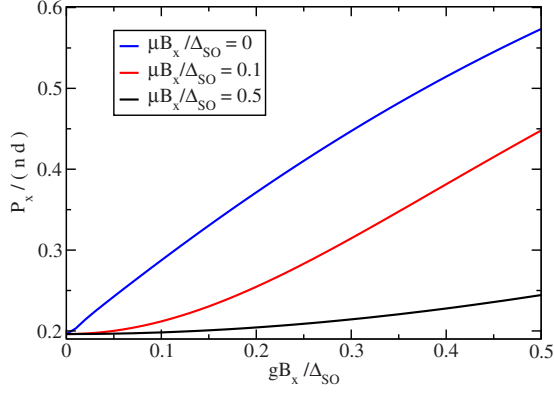
FIG. 14. (Color online) Electric polarization P_x (x component) in Eq. (134) as a function of the magnetic field in the x direction. The three lines correspond to various values of an additional external electric field in the z direction. The plot is for the temperature $k_BT = 0.001\Delta_{SO}$, and the electric field $dE_x = 0.1\Delta_{SO}$.

polarization P_i ranges from being independent of the magnitude of the electric field ($\mathcal{E} \ll \mathcal{B}$) to a linear dependence on the applied electric field E for large fields ($\mathcal{E} \gg \mathcal{B}$). Also, the polarization is strongly dependent on the magnetic field (linear in B) for low E fields, thus implying strong magnetoelectric response.

We now switch to the other special case, namely, when the external magnetic field is applied perpendicularly to the spin triangles. The electric polarization now reads

$$P_i = \frac{nd\mathcal{E}_i}{4\Delta_{\mathcal{E}}}\tanh(\beta\Delta_{\mathcal{E}}), \qquad (141)$$

with $\Delta_{\mathcal{E}} = \sqrt{\Delta_{SO}^2 + \mathcal{E}^2}$. The polarization P_i does not depend on the magnetic field B, and there are no spin-electric effects present for this particular case.

Our results suggest that the spin-electric coupling can be detected by measuring the polarization of the crystal of triangular single molecule antiferromagnets that lie in parallel planes in the in-plane electric and magnetic fields.
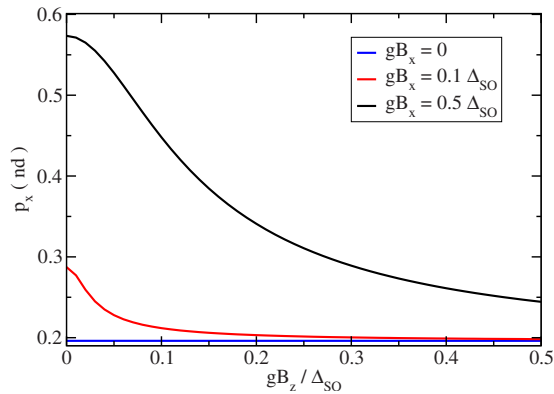

FIG. 15. (Color online) Electric polarization P_x (x component) in Eq. (134) as a function of the magnetic field in the z direction. The three lines correspond to various values of the external magnetic field in the x direction. The plot is for the temperature $k_BT = 0.001\Delta_{SO}$, and the electric field $dE_x = 0.1\Delta_{SO}$.
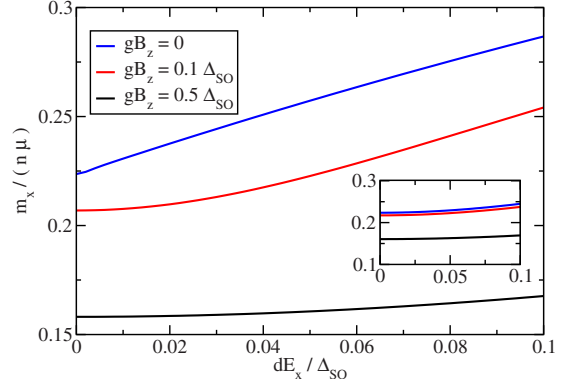

FIG. 16. (Color online) In-plane magnetization M_x in the x direction in Eq. (135) as a function of the electric field E_x in the x direction. The three lines correspond to a fixed value of an additional magnetic field in the z direction. The assumed temperature is $k_BT = 0.001\Delta_{SO}$, while in the inset it is at higher temperature $k_BT = 0.1\Delta_{SO}$.

The out-of plane component M_z of the molecule's magnetization is rather insensitive to the electric fields since any effect of the applied in-plane electric field has to compete with the spin-orbit coupling induced zero-field splitting Δ_{SO}. Since we expect to find weak coupling to electric field and small coupling constant d, it would require very strong electric fields to achieve the regime $d|\mathbf{E}| \sim \Delta_{SO}$. The in-plane components of magnetization M_x and M_y, on the other hand, show clear dependence on electric fields, Fig. 16. At low magnetic fields the in-plane component of polarization appears and grows with the strength of in-plane electric fields. However, the electric field dependence becomes less pronounced when an additional magnetic field is applied normal to the triangle's plane.

In the dependence of the magnetization on electric fields, and for the case of an in-plane magnetic field, we find the same two main regimes as in the study of the polarization: $\mathcal{E} \gg k_BT$ (i) and $\mathcal{E} \ll k_BT$ (ii). In the first case (i) we obtain

$$M_i \simeq \frac{ng_i\mu_B\mathcal{B}_i}{4\Delta_{\mathcal{B}}}\left(1 + \frac{\mathcal{E}\Delta_{SO}^2}{\mathcal{B}\Delta_{\mathcal{B}}^2}\right), \qquad (142)$$

while for the second case (ii) we get

$$M_i = \frac{ng_\perp\mu_B\mathcal{B}_i}{4\Delta_{\mathcal{B}}}\left[1 - \frac{3\mathcal{E}^2\Delta_{SO}^2}{2\Delta_{\mathcal{B}}^4}\left(1 - \frac{\beta\Delta_{\mathcal{B}}}{3}\right)\right]. \qquad (143)$$

The magnetization shows a strong dependence on the electric field E, especially for $\mathcal{E} \gg \mathcal{B}$ where this is linear in E field. For low electric fields, however, the magnetization shows only a weak dependence on the electric field, both at low and high temperatures.

For the magnetization (along z) in the presence of a perpendicular (also along z) magnetic field we obtain

$$M_z = \frac{ng_z\mu_B}{4}\tanh(\beta\mathcal{B}), \qquad (144)$$

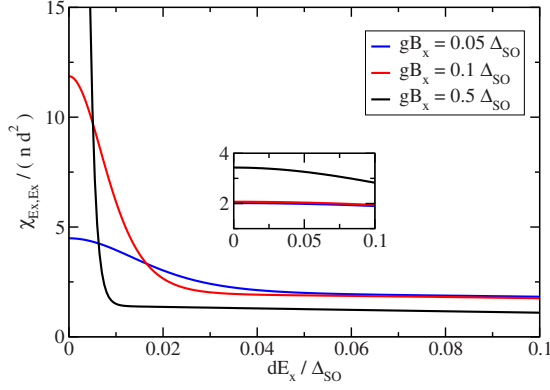which is manifestly independent of the spin-electric coupling constant d.

FIG. 17. (Color online) Electric susceptibility (*xx* component), Eq. (136), as a function of the electric field in *x* direction. The three lines correspond to various values of the external magnetic field in the *x* direction. The plot is for the temperature $k_\mathrm{B}T = 0.001\Delta_\mathrm{SO}$. In the inset, the same quantity is plotted at a higher temperature, $k_\mathrm{B}T = 0.1\Delta_\mathrm{SO}$.

2. Susceptibilities

The effects of spin-electric coupling on the polarization of a molecule show up in the electric susceptibility and the spin-electric susceptibility. In Figs. 17 and 18, we plot the *xx* and *xy* components of the electric susceptibility tensor as a function of electric field for various strengths and orientations of an additional magnetic field. Both susceptibilities show a high peak in the region of weak electric fields that is suppressed by in-plane magnetic fields. The peaks are pronounced at low temperatures and vanish as the temperature exceeds the splitting of the two lowest-energy levels, $k_\mathrm{B}T \gg d|\mathbf{E}_\parallel|$.

In the case of in-plane magnetic field, and weak coupling to the electric field $d|\mathbf{E}| \ll \Delta_\mathrm{SO}$, we can calculate the electric $\chi_{E_i E_j}$ and spin-electric $\chi_{E_i B_j}$ susceptibilities in the two limiting cases (i) and (ii) defined above, with $i = x, y$. For the electric susceptibility we obtain
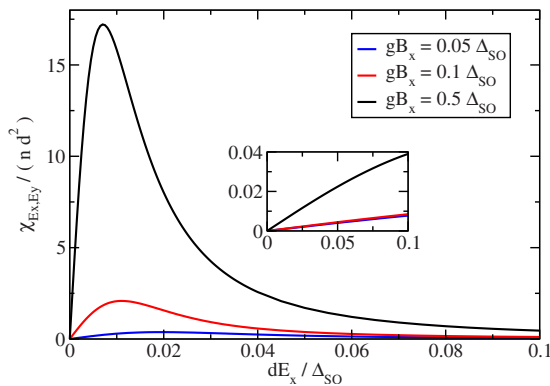

FIG. 18. (Color online) Electric susceptibility (*xy* component), Eq. (136), as a function of the electric field in *x* direction. The three lines correspond to various values of the external magnetic field in the *x* direction. The plot is for the temperature $k_\mathrm{B}T = 0.001\Delta_\mathrm{SO}$. In the inset the same quantity is plotted at a higher temperature $k_\mathrm{B}T = 0.1\Delta_\mathrm{SO}$.

$$\chi_{E_i E_j} \simeq \begin{cases} \dfrac{nd^2\mathcal{B}(\mathcal{E}^2 \delta_{ij} - \mathcal{E}_i\mathcal{E}_j)}{4\mathcal{E}^3\Delta_\mathcal{B}} & \text{for } \mathcal{E} \ll \mathcal{B} \\[2mm] \dfrac{nd^2\Delta_\mathrm{SO}^2 \delta_{ij}}{4\Delta_\mathcal{B}^3} & \text{for } \mathcal{E} \gg \mathcal{B} \end{cases} \tag{145}$$

in the first case (i), and

$$\chi_{E_i E_j} \simeq \frac{nd\Delta_\mathrm{SO}^2 \delta_{ij}}{4\Delta_\mathcal{B}^3}\left(1 + \frac{\mathcal{B}^2}{\Delta_\mathrm{SO}^2}\beta\Delta_\mathcal{B}\right). \tag{146}$$

in the second case (ii). We see that for low *E* fields, the electric susceptibility $\chi_{E_i E_j}$ depends strongly on the applied electric field, and even vanishes if the field is applied, say, along the *x* or *y* directions. For large *E* fields instead, the electric susceptibility becomes independent of the electric field itself and, for low magnetic fields (i.e., for $\mathcal{B} \ll \Delta_\mathrm{SO}$) this reduces to a constant value $\chi_{E_i E_j} = \delta_{ij}nd^2/4\Delta_\mathrm{SO}$. At finite (large) temperatures the electric susceptibility is still independent of the electric field, but it is enhanced by thermal effects $\sim 1/T$.

For the electric susceptibilities $\chi_{E_i E_j}$ in perpendicular magnetic field, we obtain

$$\chi_{E_i E_j} = \frac{nd^2}{4\Delta_\mathcal{E}}\left(\delta_{ij} - \frac{\mathcal{E}_i\mathcal{E}_j}{\Delta_\mathcal{E}}\right), \tag{147}$$

where we assumed $\Delta_\mathrm{SO} \gg k_\mathrm{B}T$, as in the previous section. As expected, there is no dependence of $\chi_{E_i E_j}$ on the *B* field, and for vanishing electric field the electric susceptibility reduces to a constant $\chi_{E_i E_j} = \delta_{ij}nd^2/4\Delta_\mathrm{SO}$.

The quantity of most interest in the present spin system is the spin-electric susceptibility $\chi_{E_i B_j}$, i.e., the magnetic response (electric response) in electric fields (magnetic fields). The nonzero spin-electric susceptibility allows for the electric control of magnetization and magnetic control of polarization in the crystals of triangular MNs, even in the case when the coupling between the molecules is negligible. In addition, $\chi_{E_i B_j}$ is nonzero only in the presence of spin-electric coupling, i.e., when $d \neq 0$.

The spin-electric susceptibility shows a characteristic peak in weak electric fields which vanishes in an external magnetic field, see Figs. 19 and 20. The peak in the diagonal *xx* component, $\chi_{E_x B_x}$, moves toward the higher electric fields and broadens as the magnetic field B_x increases. The peak in the off-diagonal component $\chi_{E_x B_z}$, on the other hand, shifts toward the lower electric fields and narrows as the in-plane magnetic field increases. Both peaks disappear at high temperatures, $k_\mathrm{B}T \gg \Delta_\mathrm{SO}$.

For in-plane magnetic fields and weak spin-electric coupling the spin-electric susceptibility $\chi_{E_i B_j}$ is

$$\chi_{E_i B_j} \simeq \frac{ndg_j\mu_B\mathcal{E}_i\mathcal{B}_j\Delta_\mathrm{SO}^2}{4\mathcal{E}\mathcal{B}\Delta_\mathcal{B}^3} \tag{148}$$

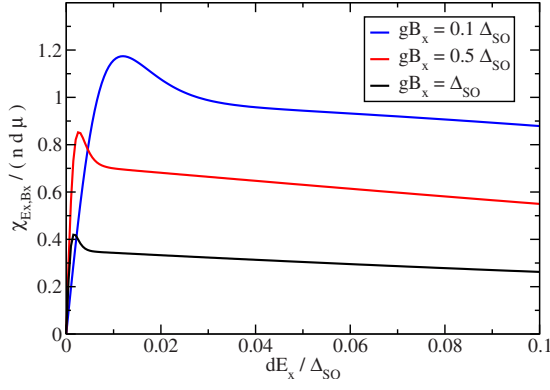for the low temperature case (i), while for the second case (ii) we obtain

FIG. 19. (Color online) Linear magnetoelectric tensor (*xx* component) in Eq. (138) as a function of the electric field in the *x* direction. The three lines correspond to various values of the external magnetic field in the *x* direction. The plot is for the temperature $k_BT=0.001\Delta_{SO}$.

$$\chi_{E_iB_j} \simeq - \frac{3n\Delta_{SO}^2 dg_j\mu_B\mathcal{E}_i\mathcal{B}_j}{4\Delta_{\mathcal{B}}^5}\left(1 - \frac{\beta\Delta_{\mathcal{B}}}{3}\right). \qquad (149)$$

By inspecting the above expression, we can infer that for low temperatures and low *E* fields the spin-electric susceptibility shows no dependence on the absolute value of the electric field *E* and only a weak dependence on the applied magnetic field *B*. Moreover, when both fields are applied along one special direction, say, along *x*, and assuming also $\mathcal{B} \ll \Delta_{SO}$, the spin-electric susceptibility becomes $\chi_{E_xB_x}=ndg_i\mu_B/4\Delta_{SO}$, i.e., it reaches a constant value. The finite temperature expression shows that the spin-electric response is reduced, as opposed to the electric response where temperature increases the response. Thus, for strong spin-electric response one should probe the spin system at low temperatures ($k_BT \ll \Delta_{SO}$) (Fig. 21).

The diagonal out-of-plane component of the magnetic susceptibility, $\chi_{B_zB_z}$, in the presence of an external magnetic field in the *x* direction decays strongly in the applied electric
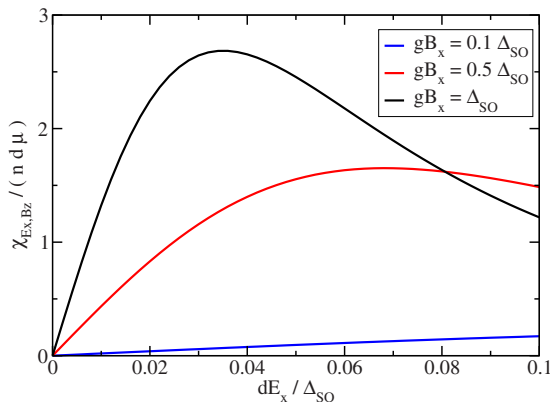

FIG. 20. (Color online) Linear magnetoelectric tensor (*xz* component) in Eq. (138) as a function of the electric field in the *x* direction. The three lines correspond to various values of the external electric field in the *x* direction. The plot is for the temperature $k_BT=0.001\Delta_{SO}$.
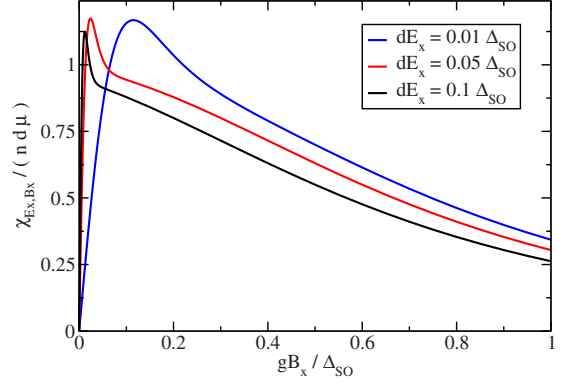

FIG. 21. (Color online) Linear magnetoelectric tensor (*xx* component) in Eq. (138) as a function of the magnetic field in the *x* direction. The three lines correspond to various values of the external electric field in the *x* direction. The plot is for the temperature $k_BT=0.001\Delta_{SO}$.

field along the *x* direction, Fig. 22. In electric fields, the $\chi_{B_xB_x}$ component shows a peak that is reduced by the application of the magnetic field in the *x* direction, Fig. 23.

We can derive the magnetic susceptibilities in the two regimes. In the first case (i) we obtain (assuming now only linear effects in *E* field)

$$\chi_{B_iB_j} = \frac{ng_\perp^2\mu_B^2}{2\Delta_{\mathcal{B}}}\left[\delta_{ij} - \frac{\mathcal{B}_i\mathcal{B}_j}{\Delta_{\mathcal{B}}^2} + \frac{\mathcal{E}\Delta_{SO}^2}{\mathcal{B}\Delta_{\mathcal{B}}^2}\left(\delta_{ij} - \frac{(3\mathcal{B}^2 + \Delta_{\mathcal{B}}^2)\mathcal{B}_i\mathcal{B}_j}{B^2\Delta_{\mathcal{B}}^2}\right)\right],$$
$$(150)$$

with $i,j=x,y$, while

$$\chi_{B_zB_z} = \frac{ng_z^2\mu_B^2}{2\Delta_{\mathcal{B}}}\frac{\Delta_{SO}^2}{\mathcal{B}\mathcal{E}} \qquad (151)$$

for $\mathcal{B}_z\Delta_{SO} \ll \mathcal{B}\mathcal{E}$. At low temperatures the in-plane magnetic susceptibility shows a linear dependence on the applied electric field *E*, thus allowing for a simple estimate of the electric dipole parameter *d* from magnetic measurements. Note that

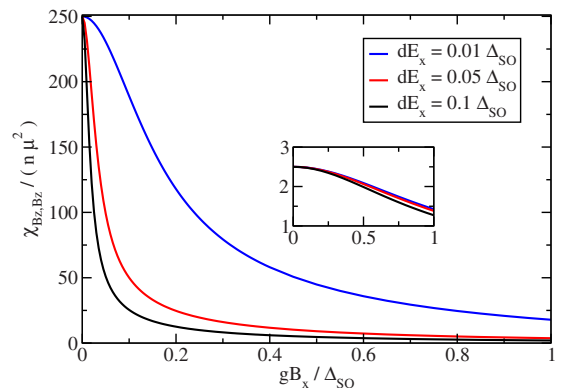
FIG. 22. (Color online) Magnetic susceptibility (*zz* component) in Eq. (137) as a function of the magnetic field in the *x* direction. The three lines correspond to various values of the external electric field in the *x* direction. The plot is for the temperature $k_BT=0.001\Delta_{SO}$. The inset represents the same quantity at a higher temperature $k_BT=0.1\Delta_{SO}$.
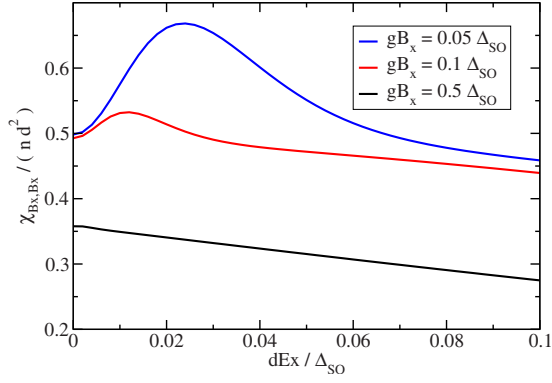
FIG. 23. (Color online) Magnetic susceptibility (xx component), Eq. (137) as a function of the electric field in the x direction. The three lines correspond to various values of the additional magnetic field in the z direction. The plot is for the temperature k_BT $=0.001\Delta_{SO}$.

for strong electric fields ($\mathcal{E} \gg \mathcal{B}$), the magnetic susceptibility can vanish since the magnetization does not depend on the magnetic field anymore. However, such a regime would not help to identify the electric dipole coupling strength d from susceptibility measurements directly. The perpendicular magnetic susceptibility shows a strong electric field dependence $\chi_{B_zB_z} \sim \mathcal{E}^{-1}$ and can be used as an efficient probe for extracting the electric dipole parameter d. In the second case (ii) we obtain

$$\chi_{B_iB_j} = \frac{ng_\perp^2\mu_B^2}{2\Delta_\mathcal{B}}\left[\delta_{ij} - \frac{\mathcal{B}_i\mathcal{B}_j}{\Delta_\mathcal{B}^2} - \frac{\mathcal{E}^2\Delta_{SO}^2}{\Delta_\mathcal{B}^4}\left(\frac{3}{2}\left(\delta_{ij} + \frac{\mathcal{B}_i\mathcal{B}_j}{\Delta_\mathcal{B}^2}\right)\right.\right.$$
$$\left.\left. - \beta\Delta_\mathcal{B}\left(\delta_{ij} + \frac{4\mathcal{B}_i\mathcal{B}_j}{\Delta_\mathcal{B}^2}\right)\right)\right], \quad (152)$$

when $i,j = x,y$, and

$$\chi_{B_zB_z} = \frac{ng_z^2\mu_B^2\mathcal{B}^2}{2\Delta_\mathcal{B}^3}\left(1 + \beta\Delta_\mathcal{B}\frac{\Delta_{SO}^2}{\mathcal{B}^2}\right). \quad (153)$$

The magnetic response increases with temperature. Also, in this limit the dependence of the magnetic susceptibility on the applied electric field is rather weak ($\chi_{B_iB_j}(\mathcal{E}) \sim \mathcal{E}^2$), thus this regime is also not suitable for observing spin-electric effects.

For the magnetic susceptibility in the perpendicular magnetic field we find

$$\chi_{B_zB_z} = \frac{\beta ng_z^2\mu_B^2}{4}\operatorname{sech}(\beta\mathcal{B}), \quad (154)$$

while for the in-plane magnetic susceptibility $\chi_{B_{x(y)}B_{x(y)}}$ we obtain

$$\chi_{B_{x(y)}B_{x(y)}} = \frac{ng_z^2\mu_B^2\Delta_{SO}}{2(\mathcal{B}^2 - \Delta_{SO}^2)}\left[\frac{\mathcal{B}}{\Delta_{SO}}\left(1 - \frac{\mathcal{E}^2}{\mathcal{B}^2}\right)\tanh(\beta\mathcal{B}) - 1\right] \quad (155)$$

in the limit $\mathcal{B}, k_BT \ll \Delta_{SO}$. We mention that for B perpendicular to the molecular plane there is no electric field E (mag-
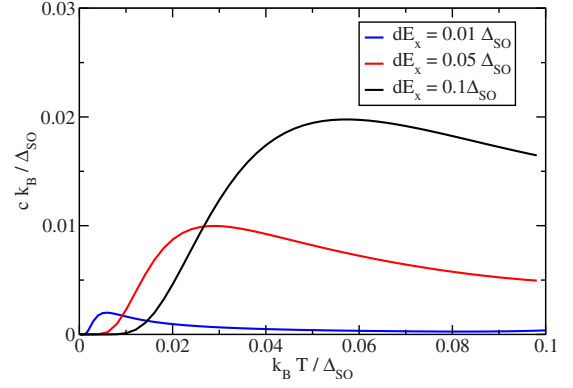
netic field B) dependence of the magnetization M_i (electric polarization P_i). Thus, in order to see spin-electric effects one needs to apply magnetic fields which have nonzero in-plane components.

FIG. 24. (Color online) Heat capacity, Eq. (156), as a function of temperature in various electric fields.

D. Heat capacity

Next we investigate the dependence of the heat capacity on the applied electric and magnetic fields in different regimes. The heat capacity is defined as $C = -\partial/\partial T(\partial \ln(Z)/\partial\beta)$ so that we obtain

$$C = \frac{Nk_B\beta^2}{4}\sum_{p=\pm 1}\frac{(E_1 + pE_{-1})^2}{\cosh^2\left[\frac{\beta(E_1 + pE_{-1})}{2}\right]}. \quad (156)$$

We consider the cases of perpendicular B field and in-plane B field in the limit $\Delta_{SO} \gg k_BT$. In the first case, i.e., for $B\|z$ we obtain

$$C \simeq Nk_B\beta^2\begin{cases}\Delta_\mathcal{E}^2 e^{-2\beta\Delta_{SO}} + \mathcal{B}^2 e^{-2\beta\mathcal{B}}, & \mathcal{B} \gg k_BT \\ \Delta_\mathcal{E}^2 e^{-2\beta\Delta_{SO}} + \dfrac{\mathcal{B}^2}{4}, & \mathcal{B} \ll k_BT.\end{cases} \quad (157)$$

The heat capacity C shows a quadratic dependence on the applied electric field for the entire range of E-field strengths. On the other hand, the magnetic field dependence of C is nonmonotonic and shows a maximum for some finite B-field strength $\mathcal{B}_{max} \simeq k_BT$. In the second situation, i.e., for $B \perp z$ we get

$$C \simeq Nk_B\beta^2\begin{cases}\dfrac{\mathcal{B}^2\mathcal{E}^2}{\Delta_\mathcal{B}^2}e^{-2(\beta\mathcal{B}\mathcal{E}/\Delta_\mathcal{B})} + \Delta_\mathcal{B}^2 e^{-2\beta\Delta_\mathcal{B}}, & \mathcal{E} \gg k_BT \\ \dfrac{\mathcal{B}^2\mathcal{E}^2}{4\Delta_\mathcal{B}^2}, & \mathcal{E} \ll k_BT.\end{cases} \quad (158)$$

As in the previous case, the dependence of the heat capacity C is linear in E field for low E fields. However, for large E fields the dependence is nonmonotonic and thus shows a maximum for some finite electric field strength $\mathcal{E}_{max} \simeq k_BT$.
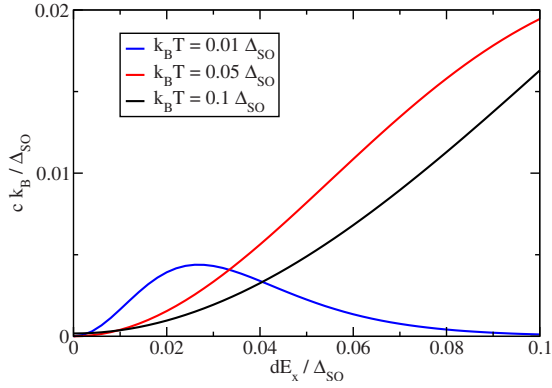
FIG. 25. (Color online) Heat capacity, Eq. (156), at low temperature as a function of external electric field.

Note that in this case also the dependence on the magnetic field is nonmonotonic, and thus we obtain a second maximum for $\mathcal{B}_{\max} \simeq k_B T$. The effects of the spin-electric coupling on the heat capacity are illustrated in Figs 24 and 25. We can conclude from the above expressions that the strongest dependence of the heat capacity on the electric field is when the magnetic field is applied in plane, and then it is mostly quadratic.

For the derivation of all the thermodynamic quantities presented in the previous sections, we have restricted ourselves to the contributions arising from only the lowest four states, even though the spin system spans eight states in total. This description is valid if the splitting between the energies of $S=1/2$ and $S=3/2$ states is much larger than the temperature $k_B T$. This splitting varies strongly with the applied magnetic field for $\mathcal{B}=3J/4$ one of the $S=3/2$ states ($M=-3/2$) crossing the $M=1/2$ of the $S=1/2$ states and, even more, for $\mathcal{B}>3J/2$ the $M=-3/2$ becomes the spin system ground states. Thus, for large magnetic fields our effective description in terms of only the $S=1/2$ states breaks down and one have to reconsider the previous quantities in this limit.

V. CONCLUSIONS

Electric fields can be applied at very short spatial and temporal scales, which makes them preferable for quantum information processing applications over the more standard magnetic fields. Molecular nanomagnets, while displaying rich quantum dynamics, have not yet been shown to respond to electric fields in experiments. We have investigated theoretically the possibility of spin-electric coupling in molecular nanomagnets using symmetry analysis and found that the spin-electric coupling is possible in antiferromagnetic ground-state manifolds of spin-1/2 and spin-3/2 triangles, as well as in spin-1/2 pentagon. The spin-electric coupling in the triangle can exist even in the absence of spin-orbit coupling, while the coupling in the pentagon requires the spin-orbit interaction in the molecule. We have characterized the form of the spin-electric coupling in all of these molecules and presented the selection rules for the transitions between the spin states induced by electric fields.

While the symmetry can predict the presence or absence of the spin-electric coupling, it cannot predict the size of the corresponding coupling constant. In order to find a molecule suitable for electric manipulation, it is necessary to have an estimate of the spin-electric coupling strength. For this purpose, we have described the molecular nanomagnets in terms of the Hubbard model and related the coupling constants of the symmetry-based models to the hopping and on-site energy parameters of the Hubbard model. We have found that the modification of the Hubbard model parameters due to the electric field produces a spin-electric coupling of the same form as predicted by the symmetry analysis. However, within the Hubbard model, the coupling constants have a clear and intuitive meaning in terms of the hopping and on-site energies of the localized electrons. We have also studied the superexchange interaction of the spins on the magnetic centers through the bridge. If we assume that the interaction of the localized spins is a property of the bridge alone, the spin-electric coupling can be calculated by *ab initio* analysis of the bridge alone, and not of the entire molecule.

Finally, we analyzed the role of spin-electric coupling in standard experimental setups typically used for the characterization of molecular nanomagnets. We find that the spin-electric coupling can be detected in the ESR and NMR spectra that probe the local spins. Also, thermodynamic quantities, like the polarization, magnetization, linear magnetoelectric effect, and the specific heat, show signatures of spin-electric coupling in the triangular molecules. Thus, our results set a path toward finding suitable molecules that exhibit spin-electric effects and how they can be identified experimentally.

In this work, we have focused on the spin rings with an odd number of magnetic centers (odd spin rings), whose low-energy spectrum is dominated by frustration effects. The odd spin rings, due to frustration, possess a fourfold degenerate ground state multiplet, which can be split by electric fields. As opposed to the odd spin rings, the ground states of even-spin rings is usually a nondegenerate $S=0$ state, separated from the higher energy states by a gap of the order of exchange coupling J. Coupling of the electric field to these states can thus proceed only via excited states, and the coupling strength is reduced by $d|\mathbf{E}|/J$. Similarly, in odd-spin rings where the spin frustration is removed by a lowered symmetry, the ground-state multiplet consists of an $S=1/2$ Kramers doublet, which cannot be split by electric fields. Therefore, the odd spin rings with equivalent magnetic centers seem to be the most suitable candidates for observing the spin-electric coupling and using it for quantum control of spins.

APPENDIX A: SPIN STATES IN TERMS OF THE $c_\Gamma^\dagger$ OPERATORS

In this appendix, we show the expressions for the three-electron symmetry-adapted states $|\psi_\Gamma^{j;\sigma}\rangle$ in Eqs. (29) and (37)

in terms of the symmetry adapted creation operators $c_{\Gamma,\sigma}^\dagger$. Making use of Eq. (46) we obtain

$$|\psi_{A_2'}^{1\sigma}\rangle = \frac{i\epsilon}{\sqrt{3}}(c_{A_1'\bar{\sigma}}^\dagger c_{E_+'\sigma}^\dagger c_{E_-'\sigma}^\dagger + c_{E_+'\bar{\sigma}}^\dagger c_{E_-'\sigma}^\dagger c_{A_1'\sigma}^\dagger - c_{E_-'\bar{\sigma}}^\dagger c_{E_+'\sigma}^\dagger c_{A_1'\sigma}^\dagger)|0\rangle,$$

$$\text{(A1)}$$

$$|\psi_{E_+'}^{1\sigma}\rangle = \frac{i}{\sqrt{3}}(c_{A_1'\bar{\sigma}}^\dagger c_{A_1'\sigma}^\dagger c_{E_+'\sigma}^\dagger + \epsilon c_{E_+'\bar{\sigma}}^\dagger c_{E_+'\sigma}^\dagger c_{E_-'\sigma}^\dagger + \bar{\epsilon} c_{E_-'\bar{\sigma}}^\dagger c_{E_-'\sigma}^\dagger c_{A_1'\sigma}^\dagger)|0\rangle,$$

$$\text{(A2)}$$

$$|\psi_{E_-'}^{1\sigma}\rangle = \frac{i}{\sqrt{3}}(c_{A_1'\bar{\sigma}}^\dagger c_{A_1'\sigma}^\dagger c_{E_-'\sigma}^\dagger + \epsilon c_{E_-'\bar{\sigma}}^\dagger c_{E_-'\sigma}^\dagger c_{E_+'\sigma}^\dagger + \bar{\epsilon} c_{E_+'\bar{\sigma}}^\dagger c_{E_+'\sigma}^\dagger c_{A_1'\sigma}^\dagger)|0\rangle,$$

$$\text{(A3)}$$

$$|\psi_{A_1'}^{2\sigma}\rangle = \frac{\sigma\epsilon}{\sqrt{2}}(c_{E_+'\bar{\sigma}}^\dagger c_{A_1'\sigma}^\dagger c_{E_-'\sigma}^\dagger + c_{E_-'\bar{\sigma}}^\dagger c_{A_1'\sigma}^\dagger c_{E_+'\sigma}^\dagger)|0\rangle, \quad \text{(A4)}$$

$$|\psi_{A_2'}^{2\sigma}\rangle = -\frac{i\sigma\epsilon}{\sqrt{6}}(2c_{A_1'\bar{\sigma}}^\dagger c_{E_+'\sigma}^\dagger c_{E_-'\sigma}^\dagger + c_{E_+'\bar{\sigma}}^\dagger c_{A_1'\sigma}^\dagger c_{E_-'\sigma}^\dagger - c_{E_-'\bar{\sigma}}^\dagger c_{A_1'\sigma}^\dagger c_{E_+'\sigma}^\dagger)$$
$$\times|0\rangle, \quad \text{(A5)}$$

$$|\psi_{E_+'1}^{2\sigma}\rangle = \frac{\sigma}{\sqrt{2}}(\bar{\epsilon} c_{A_1'\bar{\sigma}}^\dagger c_{A_1'\sigma}^\dagger c_{E_+'\sigma}^\dagger + \epsilon c_{E_-'\bar{\sigma}}^\dagger c_{A_1'\sigma}^\dagger c_{E_-'\sigma}^\dagger)|0\rangle, \quad \text{(A6)}$$

$$|\psi_{E_-'1}^{2\sigma}\rangle = \frac{\sigma}{\sqrt{2}}(\bar{\epsilon} c_{A_1'\bar{\sigma}}^\dagger c_{A_1'\sigma}^\dagger c_{E_-'\sigma}^\dagger + \epsilon c_{E_+'\bar{\sigma}}^\dagger c_{A_1'\sigma}^\dagger c_{E_+'\sigma}^\dagger)|0\rangle, \quad \text{(A7)}$$

$$|\psi_{E_+'2}^{2\sigma}\rangle = \frac{i\sigma\bar{\epsilon}}{\sqrt{6}}(c_{A_1'\bar{\sigma}}^\dagger c_{A_1'\sigma}^\dagger c_{E_+'\sigma}^\dagger - \bar{\epsilon} c_{E_-'\bar{\sigma}}^\dagger c_{A_1'\sigma}^\dagger c_{E_-'\sigma}^\dagger - 2\epsilon c_{E_+'\bar{\sigma}}^\dagger c_{E_+'\sigma}^\dagger c_{E_-'\sigma}^\dagger)$$
$$\times|0\rangle, \quad \text{(A8)}$$

$$|\psi_{E_-'2}^{2\sigma}\rangle = \frac{i\sigma\bar{\epsilon}}{\sqrt{6}}(c_{A_1'\bar{\sigma}}^\dagger c_{A_1'\sigma}^\dagger c_{E_-'\sigma}^\dagger - \bar{\epsilon} c_{E_+'\bar{\sigma}}^\dagger c_{A_1'\sigma}^\dagger c_{E_+'\sigma}^\dagger - 2\epsilon c_{E_-'\bar{\sigma}}^\dagger c_{E_-'\sigma}^\dagger c_{E_+'\sigma}^\dagger)$$
$$\times|0\rangle, \quad \text{(A9)}$$

where σ stands above for sign(σ).

APPENDIX B: H_{SO}, H_{e-d}^0, AND H_{e-d}^1 MATRIX ELEMENTS

For the SOI matrix elements we obtain

$$\langle\psi_{A_1'}^{2\sigma}|H_{SO}|\psi_{A_2'}^{1\sigma}\rangle = \frac{2i\lambda_{SO}}{\sqrt{2}}\sigma, \quad \text{(B1)}$$

$$\langle\psi_{E_\pm'1}^{2\sigma}|H_{SO}|\psi_{E_\pm'}^{1\sigma}\rangle = \pm\frac{i\bar{\epsilon}\lambda_{SO}}{\sqrt{2}}\sigma, \quad \text{(B2)}$$

$$\langle\psi_{E_\pm'2}^{2\sigma}|H_{SO}|\psi_{E_\pm'}^{1\sigma}\rangle = \pm\frac{\sqrt{3}\epsilon\lambda_{SO}}{\sqrt{2}}\sigma, \quad \text{(B3)}$$

$$\langle\psi_{A_1'}^{2\sigma}|H_{SO}|\psi_{A_2'}^{2\sigma}\rangle = -\sigma2\lambda_{SO}, \quad \text{(B4)}$$

$$\langle\psi_{E_\pm'1}^{2\sigma}|H_{SO}|\psi_{E_\pm'1}^{2\sigma}\rangle = \pm\sigma\frac{\sqrt{3}}{2}\lambda_{SO}, \quad \text{(B5)}$$

$$\langle\psi_{E_\pm'1}^{2\sigma}|H_{SO}|\psi_{E_\pm'2}^{2\sigma}\rangle = \pm\frac{i\lambda_{SO}}{2}\sigma, \quad \text{(B6)}$$

$$\langle\psi_{E_\pm'2}^{2\sigma}|H_{SO}|\psi_{E_\pm'2}^{2\sigma}\rangle = \mp\sigma\frac{\sqrt{3}}{2}\lambda_{SO}, \quad \text{(B7)}$$

while the remaining terms are equal to zero. For the electric dipole matrix elements we obtain

$$\langle\psi_{E_-'1}^{2\sigma}|H_{e-d}^0|\psi_{E_+'1}^{2\sigma}\rangle = \frac{a}{2}((\bar{\epsilon}-1)E_x + \epsilon\sqrt{3}E_y), \quad \text{(B8)}$$

$$\langle\psi_{E_-'2}^{2\sigma}|H_{e-d}^0|\psi_{E_+'2}^{2\sigma}\rangle = \frac{a}{2}\left(\epsilon E_x + \frac{1-\bar{\epsilon}}{\sqrt{3}}E_y\right), \quad \text{(B9)}$$

$$\langle\psi_{E_-'1}^{2\sigma}|H_{e-d}^0|\psi_{E_+'2}^{2\sigma}\rangle = -\frac{a}{2}\left(\epsilon E_x + \frac{1-\bar{\epsilon}}{\sqrt{3}}E_y\right), \quad \text{(B10)}$$

$$\langle\psi_{E_-'2}^{2\sigma}|H_{e-d}^0|\psi_{E_+'1}^{2\sigma}\rangle = -\frac{a}{2}((\bar{\epsilon}-1)E_x + \epsilon\sqrt{3}E_y), \quad \text{(B11)}$$

$$\langle\psi_{E_-'}^{1\sigma}|H_{e-d}^1|\psi_{E_+'1}^{2\sigma}\rangle = -\frac{i\epsilon E}{\sqrt{6}}(\epsilon d_{EE}^* - 2\bar{\epsilon}d_{AE}^* - d_{AE}), \quad \text{(B12)}$$

$$\langle\psi_{E_+'}^{1\sigma}|H_{e-d}^1|\psi_{E_-'1}^{2\sigma}\rangle = \frac{i\epsilon\bar{E}}{\sqrt{6}}(\epsilon d_{EE} + 2\bar{\epsilon}d_{AE}^* + d_{AE}), \quad \text{(B13)}$$

$$\langle\psi_{E_-'}^{1\sigma}|H_{e-d}^1|\psi_{E_+'2}^{2\sigma}\rangle = \frac{\epsilon E}{\sqrt{2}}(\epsilon d_{EE}^* + d_{AE}), \quad \text{(B14)}$$

$$\langle\psi_{E_+'}^{1\sigma}|H_{e-d}^1|\psi_{E_-'2}^{2\sigma}\rangle = -\frac{\epsilon\bar{E}}{\sqrt{2}}(\epsilon d_{EE} - d_{AE}), \quad \text{(B15)}$$

$$\langle\psi_{E_-'}^{1\sigma}|H_{e-d}^1|\psi_{E_+'1}^{1\sigma}\rangle = 0. \quad \text{(B16)}$$

[1] D. Gatteschi, R. Sessoli, and J. Villain, *Molecular Nanomagnets* (Oxford University Press, Oxford, 2006).

[2] D. Gatteschi and R. Sessoli, Angew. Chem., Int. Ed. **42**, 268 (2003).

[3] M. Leuenberger and D. Loss, Nature (London) **410**, 789 (2001).

[4] E. M. Chudnovsky and L. Gunther, Phys. Rev. Lett. **60**, 661 (1988).

[5] D. D. Awschalom, J. F. Smyth, G. Grinstein, D. P. DiVincenzo, and D. Loss, Phys. Rev. Lett. **68**, 3092 (1992).

[6] R. Sessoli, D. Gatteschi, A. Caneschi, and M. A. Novak, Nature (London) **365**, 141 (1993).

[7] L. Thomas, F. Lionti, R. Ballou, D. Gatteschi, R. Sessoli, and B. Barbara, Nature (London) **383**, 145 (1996).

[8] J. R. Friedman, M. P. Sarachik, J. Tejada, and R. Ziolo, Phys. Rev. Lett. **76**, 3830 (1996).

[9] W. Wernsdorfer, E. Bonet Orozco, K. Hasselbach, A. Benoit, D. Mailly, O. Kubo, H. Nakano, and B. Barbara, Phys. Rev. Lett. **79**, 4014 (1997).

[10] J. Tejada, X. X. Zhang, E. del Barco, J. M. Hernández, and E. M. Chudnovsky, Phys. Rev. Lett. **79**, 1754 (1997).

[11] E. del Barco, A. D. Kent, E. M. Rumberger, D. N. Hendrickson, and G. Christou, Phys. Rev. Lett. **91**, 047203 (2003).

[12] D. Gatteschi, A. Caneschi, L. Pardi, and R. Sessoli, Science **265**, 1054 (1994).

[13] C. Sangregorio, T. Ohm, C. Paulsen, R. Sessoli, and D. Gatteschi, Phys. Rev. Lett. **78**, 4645 (1997).

[14] D. Gatteschi, R. Sessoli, and A. Cornia, Chem. Commun. (Cambridge) (2000) 725.

[15] A. Chiolero and D. Loss, Phys. Rev. Lett. **80**, 169 (1998).

[16] F. Meier and D. Loss, Phys. Rev. Lett. **86**, 5373 (2001).

[17] M. N. Leuenberger and D. Loss, Phys. Rev. B **61**, 12200 (2000).

[18] I. Chiorescu, W. Wernsdorfer, A. Müller, H. Bögge, and B. Barbara, Phys. Rev. Lett. **84**, 3454 (2000).

[19] I. Chiorescu, W. Wernsdorfer, A. Mller, H. Bgge, and B. Barbara, J. Magn. Magn. Mater. **221**, 103 (2000).

[20] O. Waldmann, R. Koch, S. Schromm, P. Müller, I. Bernt, and R. W. Saalfrank, Phys. Rev. Lett. **89**, 246401 (2002).

[21] D. Loss, D. P. DiVincenzo, and G. Grinstein, Phys. Rev. Lett. **69**, 3232 (1992).

[22] M. N. Leuenberger and D. Loss, Phys. Rev. B **61**, 1286 (2000).

[23] M. N. Leuenberger, F. Meier, and D. Loss, Monatsch. Chem. **134**, 217 (2003).

[24] W. Wernsdorfer and R. Sessoli, Science **284**, 133 (1999).

[25] M. N. Leuenberger and D. Loss, Phys. Rev. B **63**, 054414 (2001).

[26] G. González and M. N. Leuenberger, Phys. Rev. Lett. **98**, 256804 (2007).

[27] G. González, M. N. Leuenberger, and E. R. Mucciolo, Phys. Rev. B **78**, 054445 (2008).

[28] F. Troiani, A. Ghirri, M. Affronte, S. Carretta, P. Santini, G. Amoretti, S. Piligkos, G. Timco, and R. E. P. Winpenny, Phys. Rev. Lett. **94**, 207208 (2005).

[29] A. Ardavan, O. Rival, J. J. L. Morton, S. J. Blundell, A. M. Tyryshkin, G. A. Timco, and R. E. P. Winpenny, Phys. Rev. Lett. **98**, 057201 (2007).

[30] S. Carretta, P. Santini, G. Amoretti, F. Troiani, and M. Affronte, Phys. Rev. B **76**, 024408 (2007).

[31] F. Meier, J. Levy, and D. Loss, Phys. Rev. B **68**, 134417 (2003).

[32] J. Lehmann, A. Gaita-Ariño, E. Coronado, and D. Loss, Nat. Nanotechnol. **2**, 312 (2007).

[33] G. A. Timco *et al.*, Nat. Nanotechnol. **4**, 173 (2008).

[34] A. Candini *et al.*, Phys. Rev. Lett. **104**, 037203 (2010).

[35] H. B. Heersche, Z. de Groot, J. A. Folk, H. S. J. van der Zant, C. Romeike, M. R. Wegewijs, L. Zobbi, D. Barreca, E. Tondello, and A. Cornia, Phys. Rev. Lett. **96**, 206801 (2006).

[36] K. Osorio, Edgar A. amd Moth-Poulsen, H. S. J. van der Zant, J. Paaske, P. Hedegrd, K. Flensberg, J. Bendix, and T. Bjrnholm, Nano Lett. **10**, 105 (2010).

[37] C. Romeike, M. R. Wegewijs, and H. Schoeller, Phys. Rev. Lett. **96**, 196805 (2006).

[38] C. Romeike, M. R. Wegewijs, W. Hofstetter, and H. Schoeller, Phys. Rev. Lett. **96**, 196601 (2006).

[39] M. N. Leuenberger and E. R. Mucciolo, Phys. Rev. Lett. **97**, 126601 (2006).

[40] L. Michalak, C. M. Canali, M. R. Pederson, M. Paulsson, and V. G. Benza, Phys. Rev. Lett. **104**, 017202 (2010).

[41] F. Troiani, M. Affronte, S. Carretta, P. Santini, and G. Amoretti, Phys. Rev. Lett. **94**, 190501 (2005).

[42] M. Trif, F. Troiani, D. Stepanenko, and D. Loss, Phys. Rev. Lett. **101**, 217201 (2008).

[43] C. F. Hirjibehedin, C. P. Lutz, and A. J. Heinrich, Science **312**, 1021 (2006).

[44] A. C. Bleszynski-Jayich, L. E. Fröberg, M. T. Björk, H. J. Trodahl, L. Samuelson, and R. M. Westervelt, Phys. Rev. B **77**, 245327 (2008).

[45] V. Srinivasa, J. Levy, and C. S. Hellberg, Phys. Rev. B **76**, 094411 (2007).

[46] V. Srinivasa and J. Levy, Phys. Rev. B **80**, 024414 (2009).

[47] A. I. Popov, D. I. Plokhov, and A. K. Zvezdin, EPL **87**, 67004 (2009).

[48] L. N. Bulaevskii, C. D. Batista, M. V. Mostovoy, and D. I. Khomskii, Phys. Rev. B **78**, 024402 (2008).

[49] B. S. Tsukerblat, *Group Theory in Chemistry and Spectroscopy: A Simple Guide to Advanced Usage* (Dover, New York, 2006).

[50] V. Bellini, A. Olivieri, and F. Manghi, Phys. Rev. B **73**, 184431 (2006).

[51] K.-Y. Choi, Y. H. Matsuda, H. Nojiri, U. Kortz, F. Hussain, A. C. Stowe, C. Ramsey, and N. S. Dalal, Phys. Rev. Lett. **96**, 107202 (2006).

[52] P. A. Angaridis, P. Baran, R. Boča, F. Cervantes-Lee, W. Haase, G. Mezel, R. G. Raptis, and R. Werner, Inorg. Chem. **41**, 2219 (2002).

[53] N. Baadji, M. Piacenza, T. Tugsuz, F. D. Sala, G. Maruccio, and S. Sanvito, Nature Mater. **8**, 813 (2009).

[54] T. Moriya, Phys. Rev. Lett. **4**, 228 (1960).

[55] L. Shekhtman, O. Entin-Wohlman, and A. Aharony, Phys. Rev. Lett. **69**, 836 (1992).

[56] T. Yildirim, A. B. Harris, O. Entin-Wohlman, and A. Aharony, Phys. Rev. Lett. **73**, 2919 (1994).

[57] I. A. Sergienko and E. Dagotto, Phys. Rev. B **73**, 094434 (2006).

[58] S. Dong, K. Yamauchi, S. Yunoki, R. Yu, S. Liang, A. Moreo, J.-M. Liu, S. Picozzi, and E. Dagotto, Phys. Rev. Lett. **103**, 127201 (2009).

[59] A. V. Postnikov, J. Kortus, and M. R. Pederson, Phys. Status Solidi B **243**, 2533 (2006).

[60] M. I. Belinsky, Chem. Phys. **361**, 137 (2009).

[61] M. I. Belinsky, Chem. Phys. **361**, 152 (2009).

[62] N. E. Bonesteel, T. M. Rice, and F. C. Zhang, Phys. Rev. Lett. **68**, 2684 (1992).

[63] J. M. Clemente-Juan, E. Coronado, A. Gaita-Arino, C. Gimenez-

Saiz, H.-U. Gudel, A. Sieber, R. Bircher, and H. Mutka, Inorg. Chem. **44**, 3389 (2005).

[64] J. Luzon, K. Bernot, I. J. Hewitt, C. E. Anson, A. K. Powell, and R. Sessoli, Phys. Rev. Lett. **100**, 247205 (2008).

[65] R. Winkler, *Spin-Orbit Coupling Effects in Two-Dimensional Electron and Hole Systems* (Springer-Verlag, Berlin, 2003).

[66] T. Moriya, Phys. Rev. **120**, 91 (1960).

[67] A. Bencini and D. Gatteschi, *EPR of Exchange Coupled Systems*

(Springer-Verlag, Berlin, 1989).

[68] E. Micotti, Y. Furukawa, K. Kumagai, S. Carretta, A. Lascialfari, F. Borsa, G. A. Timco, and R. E. P. Winpenny, Phys. Rev. Lett. **97**, 267204 (2006).

[69] A. Ghirri, G. Lorusso, F. Moro, F. Troiani, V. Corradini, C. Muryn, F. Tuna, G. Timco, R. E. P. Winpenny, and M. Affronte, Phys. Rev. B **79**, 224430 (2009).